



Article

A Novel Technique for Solving the Nonlinear Fractional-Order Smoking Model

Abdelhamid Mohammed Djaouti ^{1,*}, Zareen A. Khan ^{2,*}, Muhammad Imran Liaqat ³ and Ashraf Al-Quran ¹

¹ Department of Mathematics and Statistics, Faculty of Sciences, King Faisal University, Hofuf 31982, Saudi Arabia; aalquran@kfu.edu.sa

² Department of Mathematical Sciences, College of Science, Princess Nourah bint Abdulrahman University, P.O. Box 84428, Riyadh 11671, Saudi Arabia

³ Abdus Salam School of Mathematical Sciences, Government College University, 68-B, New Muslim Town, Lahore 54600, Pakistan; imran_liaqat_22@sms.edu.pk

* Correspondence: adjaout@kfu.edu.sa (A.M.D.); zakhan@pnu.edu.sa (Z.A.K.)

Abstract: In the study of biological systems, nonlinear models are commonly employed, although exact solutions are often unattainable. Therefore, it is imperative to develop techniques that offer approximate solutions. This study utilizes the Elzaki residual power series method (ERPSM) to analyze the fractional nonlinear smoking model concerning the Caputo derivative. The outcomes of the proposed technique exhibit good agreement with the Laplace decomposition method, demonstrating that our technique is an excellent alternative to various series solution methods. Our approach utilizes the simple limit principle at zero, making it the easiest way to extract series solutions, while variational iteration, Adomian decomposition, and homotopy perturbation methods require integration. Moreover, our technique is also superior to the residual method by eliminating the need for derivatives, as fractional integration and differentiation are particularly challenging in fractional contexts. Significantly, our technique is simpler than other series solution techniques by not relying on Adomian's and He's polynomials, thereby offering a more efficient way of solving nonlinear problems.

Keywords: Caputo derivative; Elzaki residual power series method; approximate solutions; fractional nonlinear smoking model



Citation: Mohammed Djaouti, A.; Khan, Z.A.; Imran Liaqat, M.; Al-Quran, A. A Novel Technique for Solving the Nonlinear Fractional-Order Smoking Model. *Fractal Fract.* **2024**, *8*, 286. <https://doi.org/10.3390/fractalfract8050286>

Academic Editor: Bipan Hazarika

Received: 3 April 2024

Revised: 3 May 2024

Accepted: 4 May 2024

Published: 10 May 2024



Copyright: © 2024 by the authors. Licensee MDPI, Basel, Switzerland. This article is an open access article distributed under the terms and conditions of the Creative Commons Attribution (CC BY) license (<https://creativecommons.org/licenses/by/4.0/>).

1. Introduction

Traditional calculus deals with integer-order derivatives and integrals, while fractional calculus (FC) extends these concepts to include derivatives and integrals of non-integer orders, such as fractional and complex orders. FC is particularly useful for modeling systems with memory effects, where the current state depends not only on the immediate past but also on past states over a longer period. This behavior is common in many physical, biological, and engineering systems, where the system retains a memory of its past states or inputs. Memory effects can arise due to various factors, such as delays, relaxation processes, and non-local interactions. FC provides a powerful mathematical framework for modeling systems with memory effects, as it allows for the incorporation of fractional-order derivatives and integrals, enabling more accurate descriptions of complex dynamics. However, in systems exhibiting memory effects, fractional-order derivatives and integrals of non-integer orders are necessary to accurately describe their dynamics. FC allows for the incorporation of memory effects by introducing fractional-order operators, such as the Riemann–Liouville, Caputo, and Grünwald–Letnikov operators. These operators generalize the classical differentiation and integration operators to handle non-integer orders, enabling the modeling of systems with long-term memory and complex dynamics. Systems with memory effects are encountered in various fields, including viscoelastic materials, biological systems, signal processing, and control theory. FC has proven to be particularly valuable in these areas, providing a flexible framework for capturing

the intricate behaviors arising from memory effects. By incorporating fractional-order derivatives and integrals, researchers can develop more accurate models and gain a better understanding of the dynamics of systems with memory [1–4].

Nonlinear fractional differential equations (NFDEs) play a crucial role in disease modeling due to their ability to capture the complex dynamics of disease progression, transmission, and intervention. Here is why they are important [5,6]:

1. **Modeling complexity:** Diseases often involve complex interactions between various biological, environmental, and social factors. NFDEs can represent these interactions more accurately than linear models, allowing for a more realistic portrayal of disease dynamics.
2. **Memory effects and long-range dependencies:** Diseases may exhibit memory effects, where past events influence future outcomes, and long-range dependencies, where distant interactions impact disease spread. Nonlinear differential equations with fractional derivatives can capture these effects, providing a better understanding of disease behavior over time and space.
3. **Nonlinearity in biological processes:** The biological processes underlying disease progression are often nonlinear, involving feedback loops, threshold effects, and complex interactions between different components of the system. NFDEs can model these nonlinearities more effectively, leading to more accurate predictions of disease outcomes.
4. **Personalized medicine:** Nonlinear models can incorporate individual variability in disease susceptibility, response to treatment, and other factors, allowing for personalized predictions and treatment strategies tailored to specific patient characteristics.
5. **Assessment of intervention strategies:** NFDEs can evaluate the effectiveness of various intervention strategies, such as vaccination campaigns, treatment protocols, and public health interventions. By simulating the impact of interventions on disease dynamics, these models can inform decision-making and resource allocation.
6. **Prediction of emergent phenomena:** Diseases may exhibit emergent phenomena such as epidemics, outbreaks, and the emergence of drug resistance. NFDEs can predict these phenomena and identify critical factors driving their occurrence, helping to design proactive measures to mitigate their impact.
7. **Integration of data:** NFDEs can integrate diverse sources of data, including epidemiological, clinical, genetic, and environmental data, to provide a comprehensive understanding of disease dynamics and inform evidence-based decision-making.

Overall, NFDEs are essential tools in disease modeling, enabling researchers to capture the complexity of disease systems and develop strategies to prevent, control, and treat diseases more effectively.

Smoking stands as one of the most significant health concerns worldwide, claiming over a million lives annually due to its detrimental impact on vital organs. Those who smoke face a heightened risk of suffering from heart attacks or developing lung cancer compared to nonsmokers. The short-term effects of smoking encompass discolored teeth, foul breath, elevated blood pressure, and persistent coughing. Conversely, the long-term consequences of smoking have recently been associated with an array of serious conditions, including stomach ulcers, lung cancer, heart disease, gum disease, throat cancer, and mouth cancer. The life expectancy of a smoker is 10–12 years less than that of a nonsmoker, and according to WHO reports, smoking causes several deaths each day. Many scientists, mathematicians, and medical professionals are working to combat smoking to protect human lives [7]. These factors have led mathematicians to attempt to create a practical smoking model.

NFDEs play a significant role in modeling smoking behavior and its implications for several reasons [8–10]:

1. **Capturing complex dynamics:** Smoking behavior is influenced by various factors such as addiction, psychological factors, social interactions, and environmental cues. NFDEs can capture the complex interactions between these factors and represent the dynamic nature of smoking behavior more accurately than traditional linear models.

2. Memory effects and long-term dependencies: Individuals' smoking behavior often exhibits memory effects, where past experiences influence current decisions, and long-term dependencies, where behavior is influenced by events far in the past. NFDEs with fractional derivatives can capture these memory effects and long-range dependencies, allowing for a more realistic representation of how past behavior influences current smoking habits.
3. Modeling addiction dynamics: Smoking addiction involves nonlinear processes such as tolerance, withdrawal symptoms, and craving cycles. NFDE models can describe these nonlinear addiction dynamics and help understand the mechanisms underlying addiction development and persistence.
4. Assessing intervention strategies: NFDE models can be used to evaluate the effectiveness of smoking cessation interventions, such as behavioral therapies, pharmacological treatments, and public health campaigns. By simulating the impact of interventions on smoking behavior dynamics, these models can help identify the most effective strategies for reducing smoking prevalence and improving public health outcomes.
5. Predicting population-level trends: NFDE models can project population-level trends in smoking prevalence, cessation rates, and smoking-related morbidity and mortality. By incorporating demographic trends, socioeconomic factors, and policy changes, these models can help policymakers anticipate future challenges and develop targeted interventions to address them.
6. Understanding heterogeneous responses: Individuals may respond differently to smoking cessation interventions due to factors such as genetics, socioeconomic, and cultural background. NFDE models can account for this heterogeneity and provide insights into how different subpopulations may respond to various interventions.

Castillo-Garsow et al. [11] introduced the initial smoking model, investigating diverse smoker categories such as potential, current, and former smokers. Drawing inspiration from these studies, numerous researchers have explored different smoking models. For example, Sharami et al. [12] adjusted Castillo-Garsow et al.'s model and introduced a new category known as chain smokers. In [13], the author introduced a modified model that numerically explores the dynamic behavior of smoking cessation. There are five categories of potential smokers: potential smokers, light smokers, smokers, quit smokers, and total smokers. His proposed model in integer order is given below:

$$\begin{aligned}
 \mathcal{D}\vartheta(\omega) &= \beta\Omega(\omega) - \delta_1\Theta(\omega)\vartheta(\omega) - (\zeta_1 + \omega)\vartheta(\omega) + \theta\Phi(\omega), \\
 \mathcal{D}\Theta(\omega) &= \delta_1\Theta(\omega)\vartheta(\omega) - \delta_2\Theta(\omega)\Psi(\omega) - (\zeta_2 + \omega)\Theta(\omega), \\
 \mathcal{D}\Psi(\omega) &= \delta_2\Theta(\omega)\Psi(\omega) - (\Upsilon + \zeta_3 + \omega)\Psi(\omega), \\
 \mathcal{D}\Phi(\omega) &= \Upsilon\Psi(\omega) - (\theta + \zeta_4 + \omega)\Phi(\omega), \\
 \mathcal{D}\Omega(\omega) &= (\beta - \omega)\Omega(\omega) - (\zeta_1\vartheta(\omega) + \zeta_2\Theta(\omega) + \zeta_3\Psi(\omega) + \zeta_4\Phi(\omega)).
 \end{aligned} \tag{1}$$

FC provides a more accurate framework for modeling complex systems with memory effects, non-local interactions, and long-range dependencies. Solutions to NFDEs allow researchers to better capture the behavior of real-world phenomena, enhancing predictive capabilities and understanding. Indeed, the inherent complexity of NFDEs often renders finding exact solutions impossible, necessitating the use of approximate methods. These equations combine the challenges of both nonlinearity and fractional-order derivatives, making them particularly difficult to solve for exact solutions. When exact solutions to NFDEs are not attainable, approximate solutions play a crucial role in understanding the behavior of systems, making predictions, and guiding engineering design and decision-making processes. In recent years, various approximate methods for solving NFDEs have been utilized [14–23].

Finding solutions to the fractional nonlinear smoking model (FNLSM) is also an interesting area for researchers. There is a range of published research on the approximate solutions (App-Ss) of the FNLSM. Haq et al. [24] used the Laplace decomposition approach

for solving FNLSM by using the Caputo derivative (CD) definition. Mahdy et al. [25] used the Mittag-Leffler function and Sumudu transform methods to find App-Ss for FNLSM utilizing the CD. Pavani and Raghavendar [26] found App-Ss to FNLSM using the Atangana-Baleanu-Caputo, Caputo-Fabrizio, and Caputo definitions with the help of the decomposition approach and the natural transform. Khan et al. [27] constructed App-Ss using the Picard approach of FNLSM with Caputo Febrizo FD. Veerasha et al. [28] established approximate and numerical solutions for the FNLSM with the q-homotopy analysis transform approach. Gunerhan et al. [29] used the differential transformation approach to find App-Ss for FNLSM. Each of these approaches has distinct restrictions and flaws. These approaches have long running periods and enormous computational demands.

In this study, App-Ss of the FNLSM are obtained using the ERPSM. The residual errors (Res-Errors) and recurrence errors (Rec-Errors) analysis, displayed in the form of graphs and numerical values, demonstrate the levels of accuracy and convergence rates of the proposed method. To assess the reliability of our technique, we compared our obtained results with those from the Laplace decomposition method (LDM) in terms of Res-Errors. The results obtained from ERPSM exhibit high agreement with the LDM [24], indicating that ERPSM is a suitable tool for solving nonlinear models of biological systems. ERPSM, on the other hand, has several advantages over other approximate series solution methods. For example, the residual power series method (RPSM) requires finding the fractional derivative each time to determine the unknown coefficients in series solutions, which is difficult in the fractional case; the variational iteration method (VIM), the adomian decomposition method (ADM), and the homotopy perturbation method (HPM) all require integration, which is also difficult in the fractional case. The great feature of the suggested method is how quickly the coefficients of terms in a series solution can be calculated using the straightforward limit concept at zero. Therefore, ERPSM has a number of advantages over other series solution methods.

Our main contributions can be outlined as follows:

1. For the first time in the literature, we have solved the smoking model using ERPSM, which offers the simplest method for determining series coefficients compared to the Adomian, homotopy, variational iteration, and residual methods.
2. We verified the correctness of our technique through analysis of Res-Errors and Rec-Errors.
3. Moreover, we compared the solutions obtained by ERPSM with those obtained by LDM. Our results strongly agree with LDM, verifying that our approach is an alternative tool for solving NFDEs.
4. To the best of our knowledge, in our research, we have solved the most modified model of smoking.

We consider the following FNLSM [24]:

$$\begin{aligned}
 \mathcal{D}^\varrho \vartheta(\omega) &= \beta\Omega(\omega) - \delta_1\Theta(\omega)\vartheta(\omega) - (\zeta_1 + \omega)\vartheta(\omega) + \theta\Phi(\omega), \\
 \mathcal{D}^\varrho \Theta(\omega) &= \delta_1\Theta(\omega)\vartheta(\omega) - \delta_2\Theta(\omega)\Psi(\omega) - (\zeta_2 + \omega)\Theta(\omega), \\
 \mathcal{D}^\varrho \Psi(\omega) &= \delta_2\Theta(\omega)\Psi(\omega) - (\Upsilon + \zeta_3 + \omega)\Psi(\omega), \\
 \mathcal{D}^\varrho \Phi(\omega) &= \Upsilon\Psi(\omega) - (\theta + \zeta_4 + \omega)\Phi(\omega), \\
 \mathcal{D}^\varrho \Omega(\omega) &= (\beta - \omega)\Omega(\omega) - (\zeta_1\vartheta(\omega) + \zeta_2\Theta(\omega) + \zeta_3\Psi(\omega) + \zeta_4\Phi(\omega)),
 \end{aligned} \tag{2}$$

subject to the conditions: $\vartheta(0) = w_1$, $\Theta(0) = w_2$, $\Psi(0) = w_3$, $\Phi(0) = w_4$, $\Omega(0) = w_5$, where, $\vartheta(\omega)$ and $\Theta(\omega)$ are potential and light smokers, respectively; $\Psi(\omega)$ represents the smoker; and $\Phi(\omega)$ and $\Omega(\omega)$, respectively, are quit smokers and total smokers at time ω . β and ω are the birth and natural birth rates, Υ is the smoking recovery rate, and δ_1 and δ_2 are the transmission coefficients. The population's rate at which a former smoker becomes a potential smoker once more is θ . The death rates of individuals $\vartheta(\omega)$, $\Theta(\omega)$, $\Psi(\omega)$, $\Phi(\omega)$, and $\Omega(\omega)$ associated with smoking disease are represented by ζ_1 , ζ_2 , ζ_3 , and ζ_4 .

Our research work is organized as follows: The subsequent section presents important definitions and lemmas that form the foundation of our study. Section 3 consists of two parts: the first part discusses the stability result, and the second part presents the primary concept of the ERPSM and establishes approximate series solutions for the FNLSM. In Section 4, we present the results obtained by ERPSM using graphics and tables. In this section, we also present a comparison study. Finally, Section 5 concludes the research work.

2. Preliminaries

This section presents the basic definitions, properties of the Elzaki transform, and lemmas relevant to the ERPSM that are used to establish approximate series and numerical solutions.

Definition 1. The Caputo fractional derivative of order $\varphi > 0$ is given by [30]:

$$D_{\omega}^{\varphi} \vartheta(\omega) = \begin{cases} \frac{1}{\Gamma(v-\varphi)} \int_0^{\omega} (\omega-p)^{v-\varphi-1} \frac{d^v}{dp^v} \vartheta(p) dp, & v-1 < \varphi < v, \\ \frac{d^v}{d\omega^v} \vartheta(\omega), & \varphi = v \in \mathbf{N}. \end{cases} \quad (3)$$

Definition 2. The Elzaki transform (ET) of $\vartheta(\omega)$ is defined as follows [31]:

$$\mathcal{Z}[\vartheta(\omega)] = \vartheta^*(\sigma) = \sigma \int_0^{\infty} \vartheta(\omega) e^{-\left(\frac{\omega}{\sigma}\right)} d\omega, \quad \varsigma_1 \leq \sigma \leq \varsigma_2, \quad (4)$$

where ς_1, ς_2 can be either finite or infinite.

Lemma 1. Consider that $\vartheta_1(\omega)$ and $\vartheta_2(\omega)$ satisfy the axioms of ET existence. Suppose that $\mathcal{Z}[\vartheta_1(\omega)] = \vartheta_1^*(\sigma)$, $\mathcal{Z}[\vartheta_2(\omega)] = \vartheta_2^*(\sigma)$ as well as the constants χ_1, χ_2 . When this occurs, the following criteria are met [32]:

- (i) $\mathcal{Z}[\chi_1 \vartheta_1(\omega) + \chi_2 \vartheta_2(\omega)] = \chi_1 \vartheta_1^*(\sigma) + \chi_2 \vartheta_2^*(\sigma)$.
- (ii) $\mathcal{Z}^{-1}[\chi_1 \vartheta_1^*(\sigma) + \chi_2 \vartheta_2^*(\sigma)] = \chi_1 \vartheta_1(\omega) + \chi_2 \vartheta_2(\omega)$,
- (iii) $\lim_{\sigma \rightarrow 0} \left(\frac{1}{\sigma^2} \vartheta(\sigma)\right) = \vartheta(0)$.
- (iv) $\mathcal{Z}[D_{\omega}^{\varphi} \vartheta(\omega)] = \frac{\vartheta^*(\sigma)}{\sigma^{\varphi}} - \sum_{\kappa=0}^{v-1} \sigma^{\kappa-\varphi+2} \vartheta^{(\kappa)}(0)$, $v-1 < \varphi \leq v$, $v \in \mathbf{N}$.
- (v) $\mathcal{Z}[D_{\omega}^{v\varphi} \vartheta(\omega)] = \frac{\vartheta^*(\sigma)}{\sigma^{v\varphi}} - \sum_{\kappa=0}^{v-1} \sigma^{\varphi(\kappa-v)+2} D_{\omega}^{\kappa\varphi} \vartheta(0)$, $0 < \varphi \leq 1$.

Lemma 2. Assume that the fractional power series (FPS) demonstration in ET space for the function $\mathcal{Z}[\vartheta(\omega)] = \vartheta^*(\sigma)$ is as follows [32]:

$$\vartheta^*(\sigma) = \sum_{v=0}^{\infty} \vartheta_v \sigma^{v\varphi+2}, \quad (5)$$

then we have

$$\vartheta_v = D_{\omega}^{v\varphi} \vartheta(0), \quad (6)$$

where $D_{\omega}^{v\varphi} = D_{\omega}^{\varphi} \cdot D_{\omega}^{\varphi} \dots D_{\omega}^{\varphi}$ (v - times).

The following theorem establishes the conditions for the $\vartheta^*(\sigma) = \sum_{v=0}^{\infty} \vartheta_v \sigma^{v\varphi+2}$ series to converge.

Lemma 3 ([33]). Let $\mathcal{Z}[\vartheta(\omega)] = \vartheta^*(\sigma)$ be represented as a new FPS in ET space.

If $|\frac{1}{\sigma^2} \mathcal{Z}[D_{\omega}^{(\kappa+1)\varphi} \vartheta(\omega)]| \leq \mathcal{S}$, then the remainder $\mathcal{R}_{\kappa}(\sigma)$ of the new form of FPS satisfies the following inequality:

$$|\mathcal{R}_{\kappa}(\sigma)| \leq \sigma^{(\kappa+1)\varphi+2} \mathcal{S}. \quad (7)$$

3. Stability Result and Algorithm of the ERPSM

The stability result and algorithm of the ERPSM are presented in this section to solve the nonlinear smoking model of fractional order.

3.1. The Stability Result for the Trivial Fixed Point

In this subsection, we are discussing the stability result at $\mathcal{E}_0(0, 0, 0, 0, 0)$. First of all, we develop the Jacobian matrix as

$$\mathcal{J} = \begin{bmatrix} \delta_1\Theta - (\zeta_1 + \omega) & -\delta_1\vartheta & 0 & \theta & \beta \\ \delta_1\Theta & \delta_1\vartheta - \delta_2\Psi - (\zeta_2 + \omega) & -\delta_2\Theta & 0 & 0 \\ 0 & \delta_2\Psi & \delta_2\Theta - (\Upsilon + \zeta_3 + \omega) & 0 & 0 \\ 0 & 0 & \Upsilon & -(\theta + \zeta_4 + \omega) & 0 \\ -\zeta_1 & -\zeta_2 & -\zeta_3 & -\zeta_4 & \beta - \omega \end{bmatrix}.$$

Stability of \mathcal{E}_0

$$\mathcal{J}(\mathcal{E}_0) = \begin{bmatrix} -(\zeta_1 + \omega) & 0 & 0 & \theta & \beta \\ 0 & -(\zeta_2 + \omega) & 0 & 0 & 0 \\ 0 & 0 & -(\Upsilon + \zeta_3 + \omega) & 0 & 0 \\ 0 & 0 & \Upsilon & -(\theta + \zeta_4 + \omega) & 0 \\ -\zeta_1 & -\zeta_2 & -\zeta_3 & -\zeta_4 & \beta - \omega \end{bmatrix}.$$

In order to determine the eigenvalues, we have to find the determinant of the above matrix, as follows:

$$\det \begin{pmatrix} -(\zeta_1 + \omega) - \mathcal{L} & 0 & 0 & \theta & \beta \\ 0 & -(\zeta_2 + \omega) - \mathcal{L} & 0 & 0 & 0 \\ 0 & 0 & -(\Upsilon + \zeta_3 + \omega) - \mathcal{L} & 0 & 0 \\ 0 & 0 & \Upsilon & -(\theta + \zeta_4 + \omega) - \mathcal{L} & 0 \\ -\zeta_1 & -\zeta_2 & -\zeta_3 & -\zeta_4 & \beta - \omega - \mathcal{L} \end{pmatrix} = 0.$$

By solving the above determinant, we have the values of the eigenvalues $\mathcal{L}_1 = -\omega$, $\mathcal{L}_2 = -(\zeta_2 + \omega)$, $\mathcal{L}_3 = -(\Upsilon + \zeta_3 + \omega)$, $\mathcal{L}_4 = -(\theta + \zeta_4 + \omega)$, $\mathcal{L}_5 = \beta - \omega - \zeta_1$. The stability of the trivial fixed point is demonstrated by the negativity of all eigenvalues.

3.2. Algorithm of the ERPSM and Series Solutions of the Nonlinear Smoking Model

This section discusses the procedure for utilizing the proposed method to obtain approximate analytical solutions to FNLSM. Initially, the ET is applied to the FNLSM, yielding an algebraic expression. Subsequently, the FPS is introduced as the ET space solution for the derived expression, constituting the fundamental principle of the ERPSM. The key distinction between the ERPSM and the RPSM lies in how the coefficients of this series are determined through the limit concept. The resultant consequences are subsequently mapped back into real space using the inverse ET. The guidelines for employing the ERPSM to identify solutions are outlined below.

Utilize \mathcal{Z} on both sides of Equation (2)

$$\begin{aligned} \mathcal{Z}[D^\varphi\vartheta(\omega)] &= \mathcal{Z}[\delta\Omega(\omega) - \delta_1\Theta(\omega)\vartheta(\omega) - (\zeta_1 + \omega)\vartheta(\omega) + \theta\Phi(\omega)], \\ \mathcal{Z}[D^\varphi\Theta(\omega)] &= \mathcal{Z}[\delta_1\Theta(\omega)\vartheta(\omega) - \delta_2\Theta(\omega)\Psi(\omega) - (\zeta_2 + \omega)\Theta(\omega)], \\ \mathcal{Z}[D^\varphi\Psi(\omega)] &= \mathcal{Z}[\delta_2\Theta(\omega)\Psi(\omega) - (\Upsilon + \zeta_3 + \omega)\Psi(\omega)], \\ \mathcal{Z}[D^\varphi\Phi(\omega)] &= \mathcal{Z}[\Upsilon\Psi(\omega) - (\theta + \zeta_4 + \omega)\Phi(\omega)], \\ \mathcal{Z}[D^\varphi\Omega(\omega)] &= \mathcal{Z}[(\beta - \omega)\Omega(\omega) - (\zeta_1\vartheta(\omega) + \zeta_2\Theta(\omega) + \zeta_3\Psi(\omega) + \zeta_4\Phi(\omega))]. \end{aligned} \quad (8)$$

For $0 < \varphi \leq 1$ from the Lemma 1(iv), we obtain the following:

$$\mathcal{Z}[D_\omega^\varphi\vartheta(\omega)] = \frac{\vartheta^*(\sigma)}{\sigma^\varphi} - \sigma^{2-\varphi}\vartheta_0. \quad (9)$$

We have also $\mathcal{Z}[\vartheta(\omega)] = \vartheta^*(\sigma)$, $\mathcal{Z}[\Theta(\omega)] = \Theta^*(\sigma)$, $\mathcal{Z}[\Psi(\omega)] = \Psi^*(\sigma)$, $\mathcal{Z}[\Phi(\omega)] = \Phi^*(\sigma)$, and $\mathcal{Z}[\Omega(\omega)] = \Omega^*(\sigma)$. Further, by taking inverse ET, we also have: $\vartheta(\omega) = \mathcal{Z}^{-1}[\vartheta^*(\sigma)]$, $\Theta(\omega) = \mathcal{Z}^{-1}[\Theta^*(\sigma)]$, $\Psi(\omega) = \mathcal{Z}^{-1}[\Psi^*(\sigma)]$, $\Phi(\omega) = \mathcal{Z}^{-1}[\Phi^*(\sigma)]$, and $\Omega(\omega) = \mathcal{Z}^{-1}[\Omega^*(\sigma)]$.

As a result, we obtain the following from Equation (8):

$$\begin{aligned}\frac{\vartheta^*(\sigma)}{\sigma^\varrho} - \sigma^{2-\varrho}\vartheta_0 &= \beta\Omega^*(\sigma) - \delta_1\mathcal{Z}[\mathcal{Z}^{-1}[\vartheta^*(\sigma)]\mathcal{Z}^{-1}[\Theta^*(\sigma)]] - (\zeta_1 + \omega)\vartheta^*(\sigma) + \theta\Phi^*(\sigma), \\ \frac{\Theta^*(\sigma)}{\sigma^\varrho} - \sigma^{2-\varrho}\Theta_0 &= \delta_1\mathcal{Z}[\mathcal{Z}^{-1}[\vartheta^*(\sigma)]\mathcal{Z}^{-1}[\Theta^*(\sigma)]] - \delta_2\mathcal{Z}[\mathcal{Z}^{-1}[\Psi^*(\sigma)]\mathcal{Z}^{-1}[\Theta^*(\sigma)]] - (\zeta_2 + \omega)\Theta^*(\sigma), \\ \frac{\Psi^*(\sigma)}{\sigma^\varrho} - \sigma^{2-\varrho}\Psi_0 &= \delta_2\mathcal{Z}[\mathcal{Z}^{-1}[\Psi^*(\sigma)]\mathcal{Z}^{-1}[\Theta^*(\sigma)]] - \sigma^\varrho(Y + \zeta_3 + \omega)\Psi^*(\sigma), \\ \frac{\Phi^*(\sigma)}{\sigma^\varrho} - \sigma^{2-\varrho}\Phi_0 &= Y\Psi^*(\sigma) - (\theta + \zeta_4 + \omega)\Phi^*(\sigma), \\ \frac{\Omega^*(\sigma)}{\sigma^\varrho} - \sigma^{2-\varrho}\Omega_0 &= (\beta - \omega)\Omega^*(\sigma) - (\zeta_1\vartheta^*(\sigma) + \zeta_2\Theta^*(\sigma) + \zeta_3\Psi^*(\sigma) + \zeta_4\Phi^*(\sigma)).\end{aligned}\quad (10)$$

From Equation (10), we have also

$$\begin{aligned}\vartheta^*(\sigma) &= \sigma^2\vartheta_0 + \sigma^\varrho\beta\Omega^*(\sigma) - \sigma^\varrho\delta_1\mathcal{Z}[\mathcal{Z}^{-1}[\vartheta^*(\sigma)]\mathcal{Z}^{-1}[\Theta^*(\sigma)]] - \sigma^\varrho(\zeta_1 + \omega)\vartheta^*(\sigma) + \sigma^\varrho\theta\Phi^*(\sigma), \\ \Theta^*(\sigma) &= \sigma^2\Theta_0 + \sigma^\varrho\delta_1\mathcal{Z}[\mathcal{Z}^{-1}[\vartheta^*(\sigma)]\mathcal{Z}^{-1}[\Theta^*(\sigma)]] - \sigma^\varrho\delta_2\mathcal{Z}[\mathcal{Z}^{-1}[\Psi^*(\sigma)]\mathcal{Z}^{-1}[\Theta^*(\sigma)]] - (\zeta_2 + \omega)\sigma^\varrho\Theta^*(\sigma), \\ \Psi^*(\sigma) &= \sigma^2\Psi_0 + \sigma^\varrho\delta_2\mathcal{Z}[\mathcal{Z}^{-1}[\Psi^*(\sigma)]\mathcal{Z}^{-1}[\Theta^*(\sigma)]] - \sigma^\varrho(Y + \zeta_3 + \omega)\Psi^*(\sigma), \\ \Phi^*(\sigma) &= \sigma^2\Phi_0 + \sigma^\varrho Y\Psi^*(\sigma) - \sigma^\varrho(\theta + \zeta_4 + \omega)\Phi^*(\sigma), \\ \Omega^*(\sigma) &= \sigma^2\Omega_0 + \sigma^\varrho(\beta - \omega)\Omega^*(\sigma) - \sigma^\varrho(\zeta_1\vartheta^*(\sigma) + \zeta_2\Theta^*(\sigma) + \zeta_3\Psi^*(\sigma) + \zeta_4\Phi^*(\sigma)).\end{aligned}\quad (11)$$

Assume that the FPS solutions of Equation (11) in ET space are below.

$$\begin{aligned}\vartheta^*(\sigma) &= \sum_{\nu=0}^{\infty} \vartheta_\nu\sigma^{2+\nu\varrho}, \quad \Theta^*(\sigma) = \sum_{\nu=0}^{\infty} \Theta_\nu\sigma^{2+\nu\varrho}, \quad \Psi^*(\sigma) = \sum_{\nu=0}^{\infty} \Psi_\nu\sigma^{2+\nu\varrho}, \quad \Phi^*(\sigma) = \sum_{\nu=0}^{\infty} \Phi_\nu\sigma^{2+\nu\varrho}, \\ \text{and } \Omega^*(\sigma) &= \sum_{\nu=0}^{\infty} \Omega_\nu\sigma^{2+\nu\varrho}.\end{aligned}$$

As a result of applying Lemma 1(iii), we obtained the following results:

$$\begin{aligned}\lim_{\sigma \rightarrow 0} \left(\frac{1}{\sigma^2}\vartheta^*(\sigma)\right) &= \vartheta_0 = w_1, \quad \lim_{\sigma \rightarrow 0} \left(\frac{1}{\sigma^2}\Theta^*(\sigma)\right) = \Theta_0 = w_2, \quad \lim_{\sigma \rightarrow 0} \left(\frac{1}{\sigma^2}\Psi^*(\sigma)\right) = \Psi_0 = w_3, \\ \lim_{\sigma \rightarrow 0} \left(\frac{1}{\sigma^2}\Phi^*(\sigma)\right) &= \Phi_0 = w_4, \quad \text{and } \lim_{\sigma \rightarrow 0} \left(\frac{1}{\sigma^2}\Omega^*(\sigma)\right) = \Omega_0 = w_5.\end{aligned}$$

Hence, FPS can be rearranged as follows:

$$\begin{aligned}\vartheta^*(\sigma) &= \vartheta_0\sigma^2 + \sum_{\nu=1}^{\infty} \vartheta_\nu\sigma^{2+\nu\varrho}, \quad \Theta^*(\sigma) = \Theta_0\sigma^2 + \sum_{\nu=1}^{\infty} \Theta_\nu\sigma^{2+\nu\varrho}, \quad \Psi^*(\sigma) = \Psi_0\sigma^2 + \sum_{\nu=1}^{\infty} \Psi_\nu\sigma^{2+\nu\varrho}, \\ \Phi^*(\sigma) &= \Phi_0\sigma^2 + \sum_{\nu=1}^{\infty} \Phi_\nu\sigma^{2+\nu\varrho}, \quad \text{and } \Omega^*(\sigma) = \Omega_0\sigma^2 + \sum_{\nu=1}^{\infty} \Omega_\nu\sigma^{2+\nu\varrho}.\end{aligned}$$

Assume that the κ th-truncated FPS solutions of Equation (11) are below.

$$\begin{aligned}\vartheta_\kappa^*(\sigma) &= \vartheta_0\sigma^2 + \sum_{\nu=1}^{\kappa} \vartheta_\nu\sigma^{2+\nu\varrho}, \quad \Theta_\kappa^*(\sigma) = \Theta_0\sigma^2 + \sum_{\nu=1}^{\kappa} \Theta_\nu\sigma^{2+\nu\varrho}, \quad \Psi_\kappa^*(\sigma) = \Psi_0\sigma^2 + \sum_{\nu=1}^{\kappa} \Psi_\nu\sigma^{2+\nu\varrho}, \\ \Phi_\kappa^*(\sigma) &= \Phi_0\sigma^2 + \sum_{\nu=1}^{\kappa} \Phi_\nu\sigma^{2+\nu\varrho}, \quad \text{and } \Omega_\kappa^*(\sigma) = \Omega_0\sigma^2 + \sum_{\nu=1}^{\kappa} \Omega_\nu\sigma^{2+\nu\varrho}, \quad \text{where } \kappa = 1, 2, 3, \dots\end{aligned}$$

The Elzaki residual functions (ERF) $\mathcal{Z}Res(\vartheta^*(\sigma))$, $\mathcal{Z}Res(\Theta^*(\sigma))$, $\mathcal{Z}Res(\Psi^*(\sigma))$, $\mathcal{Z}Res(\Phi^*(\sigma))$ and $\mathcal{Z}Res(\Omega^*(\sigma))$ for the Equation (11) are defined as follows:

$$\begin{aligned}\mathcal{Z}Res(\vartheta^*(\sigma)) &= \vartheta^*(\sigma) - \sigma^2\vartheta_0 - \sigma^\varrho\beta\Omega^*(\sigma) + \sigma^\varrho\delta_1\mathcal{Z}[\mathcal{Z}^{-1}[\vartheta^*(\sigma)]\mathcal{Z}^{-1}[\Theta^*(\sigma)]] + \sigma^\varrho(\zeta_1 + \omega)\vartheta^*(\sigma) - \\ &\quad \sigma^\varrho\theta\Phi^*(\sigma), \\ \mathcal{Z}Res(\Theta^*(\sigma)) &= \Theta^*(\sigma) - \sigma^2\Theta_0 + \sigma^\varrho\delta_1\mathcal{Z}[\mathcal{Z}^{-1}[\vartheta^*(\sigma)]\mathcal{Z}^{-1}[\Theta^*(\sigma)]] + \sigma^\varrho\delta_2\mathcal{Z}[\mathcal{Z}^{-1}[\Psi^*(\sigma)]\mathcal{Z}^{-1}[\Theta^*(\sigma)]] + \\ &\quad (\zeta_2 + \omega)\sigma^\varrho\Theta^*(\sigma), \\ \mathcal{Z}Res(\Psi^*(\sigma)) &= \Psi^*(\sigma) - \sigma^2\Psi_0 - \sigma^\varrho\delta_2\mathcal{Z}[\mathcal{Z}^{-1}[\Psi^*(\sigma)]\mathcal{Z}^{-1}[\Theta^*(\sigma)]] + \sigma^\varrho(Y + \zeta_3 + \omega)\Psi^*(\sigma), \\ \mathcal{Z}Res(\Phi^*(\sigma)) &= \Phi^*(\sigma) - \sigma^2\Phi_0 - \sigma^\varrho Y\Psi^*(\sigma) + \sigma^\varrho(\theta - \zeta_4 + \omega)\Phi^*(\sigma), \\ \mathcal{Z}Res(\Omega^*(\sigma)) &= \Omega^*(\sigma) - \sigma^2\Omega_0 + \sigma^\varrho(\beta - \omega)\Omega^*(\sigma) + \sigma^\varrho(\zeta_1\vartheta^*(\sigma) + \zeta_2\Theta^*(\sigma) - \zeta_3\Psi^*(\sigma) + \zeta_4\Phi^*(\sigma)).\end{aligned}\quad (12)$$

The κ th-ERF $\mathcal{Z}Res_\kappa(\vartheta^*(\sigma))$, $\mathcal{Z}Res_\kappa(\Theta^*(\sigma))$, $\mathcal{Z}Res_\kappa(\Psi^*(\sigma))$, $\mathcal{Z}Res_\kappa(\Phi^*(\sigma))$, and $\mathcal{Z}Res_\kappa(\Omega^*(\sigma))$ are now defined for Equation (11):

$$\begin{aligned}
 \mathcal{Z}Res_{\kappa}(\vartheta^*(\sigma)) &= \vartheta_{\kappa}^*(\sigma) - \sigma^2\vartheta_0 - \sigma^{\wp}\beta\Omega_{\kappa}^*(\sigma) + \sigma^{\wp}\delta_1\mathcal{Z}[\mathcal{Z}^{-1}[\vartheta_{\kappa}^*(\sigma)]\mathcal{Z}^{-1}[\Theta_{\kappa}^*(\sigma)]] + \sigma^{\wp}(\zeta_1 + \omega)\vartheta_{\kappa}^*(\sigma) - \\
 &\quad \sigma^{\wp}\theta\Phi_{\kappa}^*(\sigma), \\
 \mathcal{Z}Res_{\kappa}(\Theta_{\kappa}^*(\sigma)) &= \Theta_{\kappa}^*(\sigma) - \sigma^2\Theta_0 + \sigma^{\wp}\delta_1\mathcal{Z}[\mathcal{Z}^{-1}[\vartheta_{\kappa}^*(\sigma)]\mathcal{Z}^{-1}[\Theta_{\kappa}^*(\sigma)]] + \sigma^{\wp}\delta_2\mathcal{Z}[\mathcal{Z}^{-1}[\Psi_{\kappa}^*(\sigma)]\mathcal{Z}^{-1}[\Theta_{\kappa}^*(\sigma)]] + \\
 &\quad (\zeta_2 + \omega)\sigma^{\wp}\Theta_{\kappa}^*(\sigma), \\
 \mathcal{Z}Res_{\kappa}(\Psi_{\kappa}^*(\sigma)) &= \Psi_{\kappa}^*(\sigma) - \sigma^2\Psi_0 - \sigma^{\wp}\delta_2\mathcal{Z}[\mathcal{Z}^{-1}[\Psi_{\kappa}^*(\sigma)]\mathcal{Z}^{-1}[\Theta_{\kappa}^*(\sigma)]] + \sigma^{\wp}(Y + \zeta_3 + \omega)\Psi_{\kappa}^*(\sigma), \\
 \mathcal{Z}Res_{\kappa}(\Phi_{\kappa}^*(\sigma)) &= \Phi_{\kappa}^*(\sigma) - \sigma^2\Phi_0 - \sigma^{\wp}Y\Psi_{\kappa}^*(\sigma) + \sigma^{\wp}(\theta - \zeta_4 + \omega)\Phi_{\kappa}^*(\sigma), \\
 \mathcal{Z}Res_{\kappa}(\Omega_{\kappa}^*(\sigma)) &= \Omega_{\kappa}^*(\sigma) - \sigma^2\Omega_0 + \sigma^{\wp}(\beta - \omega)\Omega_{\kappa}^*(\sigma) + \sigma^{\wp}(\zeta_1\vartheta_{\kappa}^*(\sigma) + \zeta_2\Theta_{\kappa}^*(\sigma) - \zeta_3\Psi_{\kappa}^*(\sigma) + \zeta_4\Phi_{\kappa}^*(\sigma)).
 \end{aligned}
 \tag{13}$$

By inserting the κ th-truncated FPS $\vartheta_{\kappa}^*(\sigma)$, $\Theta_{\kappa}^*(\sigma)$, $\Psi_{\kappa}^*(\sigma)$, $\Phi_{\kappa}^*(\sigma)$, and $\Omega_{\kappa}^*(\sigma)$ into Equation (13), multiplying the resulting expression by $\frac{1}{\sigma^{2+\kappa\wp}}$ on both sides, and finally putting $\lim_{\sigma \rightarrow 0}$, the obtained results are as follows:

$$\begin{aligned}
 \lim_{\sigma \rightarrow 0} \left(\frac{1}{\sigma^{2+\kappa\wp}} \mathcal{Z}Res\vartheta_{\kappa}^*(\sigma) \right) &= 0, \\
 \lim_{\sigma \rightarrow 0} \left(\frac{1}{\sigma^{2+\kappa\wp}} \mathcal{Z}Res\Theta_{\kappa}^*(\sigma) \right) &= 0, \\
 \lim_{\sigma \rightarrow 0} \left(\frac{1}{\sigma^{2+\kappa\wp}} \mathcal{Z}Res\Psi_{\kappa}^*(\sigma) \right) &= 0, \\
 \lim_{\sigma \rightarrow 0} \left(\frac{1}{\sigma^{2+\kappa\wp}} \mathcal{Z}Res\Phi_{\kappa}^*(\sigma) \right) &= 0, \\
 \lim_{\sigma \rightarrow 0} \left(\frac{1}{\sigma^{2+\kappa\wp}} \mathcal{Z}Res\Omega_{\kappa}^*(\sigma) \right) &= 0.
 \end{aligned}
 \tag{14}$$

To determine the first unknown coefficient of the FPS solution, solve Equation (14) for $\kappa = 1$. The detailed methodology used to find ϑ_1 , Θ_1 , Ψ_1 , Φ_1 , and Ω_1 is outlined in the Appendix A.

$$\begin{aligned}
 \vartheta_1 &= \beta\Omega_0 - \delta_1\Theta_0\vartheta_0 - (\zeta_1 + \omega)\vartheta_0 + \theta\Phi_0, \\
 \Theta_1 &= \delta_1\Theta_0\vartheta_0 - \delta_2\Theta_0\Psi_0 - (\zeta_2 + \omega)\Theta_0, \\
 \Psi_1 &= \delta_2\Theta_0\Psi_0 - (Y + \zeta_3 + \omega)\Psi_0, \\
 \Phi_1 &= Y\Psi_0 - (\theta + \zeta_4 + \omega)\Phi_0, \\
 \Omega_1 &= (\beta - \omega)\Omega_0 - (\zeta_1\vartheta_0 + \zeta_2\Theta_0 + \zeta_3\Psi_0 + \zeta_4\Phi_0).
 \end{aligned}
 \tag{15}$$

For $\kappa = 2$ solve the Equation (14) to obtain the 2nd unknown coefficient of the FPS solution.

$$\begin{aligned}
 \vartheta_2 &= \beta\Omega_1 - \delta_1(\Theta_0\vartheta_1 + \Theta_1\vartheta_0) - (\zeta_1 + \omega)\vartheta_1 + \theta\Phi_1, \\
 \Theta_2 &= \delta_1(\Theta_0\vartheta_1 + \Theta_1\vartheta_0) - \delta_2(\Theta_0\Psi_1 + \Theta_1\Psi_0) - (\zeta_2 + \omega)\Theta_1, \\
 \Psi_2 &= \delta_2(\Theta_1\Psi_0 + \Theta_0\Psi_1) - (Y + \zeta_3 + \omega)\Psi_1, \\
 \Phi_2 &= Y\Psi_1 - (\theta + \zeta_4 + \omega)\Phi_1, \\
 \Omega_2 &= (\beta - \omega)\Omega_1 - (\zeta_1\vartheta_1 + \zeta_2\Theta_1 + \zeta_3\Psi_1 + \zeta_4\Phi_1).
 \end{aligned}
 \tag{16}$$

To find the 3rd unknown coefficient of the FPS solution, solve Equation (14) for $\kappa = 3$.

$$\begin{aligned}
 \vartheta_3 &= \beta\Omega_2 - \delta_1(\Theta_0\vartheta_2 + \Theta_1\vartheta_1 + \Theta_2\vartheta_0) - (\zeta_1 + \omega)\vartheta_2 + \theta\Phi_2, \\
 \Theta_3 &= \delta_1(\Theta_0\vartheta_2 + \Theta_1\vartheta_1 + \Theta_2\vartheta_0) - \delta_2(\Theta_0\Psi_2 + \Theta_1\Psi_1 + \Theta_2\Psi_0) - (\zeta_2 + \omega)\Theta_2, \\
 \Psi_3 &= \delta_2(\Theta_0\Psi_2 + \Theta_1\Psi_1 + \Theta_2\Psi_0) - (Y + \zeta_3 + \omega)\Psi_2, \\
 \Phi_3 &= Y\Psi_2 - (\theta + \zeta_4 + \omega)\Phi_2, \\
 \Omega_3 &= (\beta - \omega)\Omega_2 - (\zeta_1\vartheta_2 + \zeta_2\Theta_2 + \zeta_3\Psi_2 + \zeta_4\Phi_2).
 \end{aligned}
 \tag{17}$$

In the same way, to find the 4th, 5th, and 6th unknown coefficients of the FPS solution, solve Equation (14) for $\kappa = 4, 5$, and 6, and finally we obtain the following results:

$$\begin{aligned}
\vartheta_4 &= \beta\Omega_3 - \delta_1(\Theta_0\vartheta_3 + \Theta_1\vartheta_2 \frac{\Gamma(3\varrho+1)}{\Gamma(\varrho+1)\Gamma(2\varrho+1)} + \Theta_2\vartheta_1 \frac{\Gamma(3\varrho+1)}{\Gamma(\varrho+1)\Gamma(2\varrho+1)} + \vartheta_0\Theta_3) - (\zeta_1 + \omega)\vartheta_3 + \\
&\quad \theta\Phi_3, \\
\Theta_4 &= \delta_1(\Theta_0\vartheta_3 + \Theta_1\vartheta_2 \frac{\Gamma(3\varrho+1)}{\Gamma(\varrho+1)\Gamma(2\varrho+1)} + \Theta_2\vartheta_1 \frac{\Gamma(3\varrho+1)}{\Gamma(\varrho+1)\Gamma(2\varrho+1)} + \vartheta_0\Theta_3) - \delta_2(\Theta_0\Psi_3 + \Theta_1\Psi_2 \\
&\quad \frac{\Gamma(3\varrho+1)}{\Gamma(\varrho+1)\Gamma(2\varrho+1)} + \Theta_2\Psi_1 \frac{\Gamma(3\varrho+1)}{\Gamma(\varrho+1)\Gamma(2\varrho+1)} + \Psi_0\Theta_3) - (\zeta_2 + \omega)\Theta_3, \\
\Psi_4 &= \delta_2(\Theta_0\Psi_3 + \Theta_1\Psi_2 \frac{\Gamma(3\varrho+1)}{\Gamma(\varrho+1)\Gamma(2\varrho+1)} + \Theta_2\Psi_1 \frac{\Gamma(3\varrho+1)}{\Gamma(\varrho+1)\Gamma(2\varrho+1)} + \Psi_0\Theta_3) - (Y + \zeta_3 + \omega)\Psi_3, \\
\Phi_4 &= Y\Psi_3 - (\theta + \zeta_4 + \omega)\Phi_3, \\
\Omega_4 &= (\beta - \omega)\Omega_3 - (\zeta_1\vartheta_3 + \zeta_2\Theta_3 + \zeta_3\Psi_3 + \zeta_4\Phi_3).
\end{aligned} \tag{18}$$

$$\begin{aligned}
\vartheta_5 &= \beta\Omega_4 - \delta_1(\Theta_0\vartheta_4 + \Theta_1\vartheta_3 \frac{\Gamma(4\varrho+1)}{\Gamma(\varrho+1)\Gamma(3\varrho+1)} + \Theta_2\vartheta_2 \frac{\Gamma(4\varrho+1)}{\Gamma(2\varrho+1)^2} + \Theta_3\vartheta_1 \frac{\Gamma(4\varrho+1)}{\Gamma(\varrho+1)\Gamma(3\varrho+1)} + \\
&\quad \vartheta_0\Theta_4) - (\zeta_1 + \omega)\vartheta_4 + \theta\Phi_4, \\
\Theta_5 &= \delta_1(\Theta_0\vartheta_4 + \Theta_1\vartheta_3 \frac{\Gamma(4\varrho+1)}{\Gamma(\varrho+1)\Gamma(3\varrho+1)} + \Theta_2\vartheta_2 \frac{\Gamma(4\varrho+1)}{\Gamma(2\varrho+1)^2} + \Theta_3\vartheta_1 \frac{\Gamma(4\varrho+1)}{\Gamma(\varrho+1)\Gamma(3\varrho+1)} + \vartheta_0\Theta_4) - \\
&\quad \delta_2(\Theta_0\Psi_4 + \Theta_1\Psi_3 \frac{\Gamma(4\varrho+1)}{\Gamma(\varrho+1)\Gamma(3\varrho+1)} + \Theta_2\Psi_2 \frac{\Gamma(4\varrho+1)}{\Gamma(2\varrho+1)^2} + \Theta_3\Psi_1 \frac{\Gamma(4\varrho+1)}{\Gamma(\varrho+1)\Gamma(3\varrho+1)} + \Psi_0\Theta_4) - \\
&\quad (\zeta_2 + \omega)\Theta_4, \\
\Psi_5 &= \delta_2(\Theta_0\Psi_4 + \Theta_1\Psi_3 \frac{\Gamma(4\varrho+1)}{\Gamma(\varrho+1)\Gamma(3\varrho+1)} + \Theta_2\Psi_2 \frac{\Gamma(4\varrho+1)}{\Gamma(2\varrho+1)^2} + \Theta_3\Psi_1 \frac{\Gamma(4\varrho+1)}{\Gamma(\varrho+1)\Gamma(3\varrho+1)} + \Psi_0\Theta_4) - \\
&\quad (Y + \zeta_3 + \omega)\Psi_4, \\
\Phi_5 &= Y\Psi_4 - (\theta + \zeta_4 + \omega)\Phi_4, \\
\Omega_5 &= (\beta - \omega)\Omega_4 - (\zeta_1\vartheta_4 + \zeta_2\Theta_4 + \zeta_3\Psi_4 + \zeta_4\Phi_4).
\end{aligned} \tag{19}$$

$$\begin{aligned}
\vartheta_6 &= \beta\Omega_5 - \delta_1(\Theta_0\vartheta_5 + \Theta_1\vartheta_4 \frac{\Gamma(5\varrho+1)}{\Gamma(\varrho+1)\Gamma(4\varrho+1)} + \Theta_2\vartheta_3 \frac{\Gamma(5\varrho+1)}{\Gamma(2\varrho+1)\Gamma(3\varrho+1)} + \\
&\quad \Theta_3\vartheta_2 \frac{\Gamma(5\varrho+1)}{\Gamma(3\varrho+1)\Gamma(2\varrho+1)} + \Theta_4\vartheta_1 \frac{\Gamma(5\varrho+1)}{\Gamma(4\varrho+1)\Gamma(\varrho+1)} + \Theta_5\vartheta_0) - (\zeta_1 + \omega)\vartheta_5 + \theta\Phi_5, \\
\Theta_6 &= \delta_1(\Theta_0\vartheta_5 + \Theta_1\vartheta_4 \frac{\Gamma(5\varrho+1)}{\Gamma(\varrho+1)\Gamma(4\varrho+1)} + \Theta_2\vartheta_3 \frac{\Gamma(5\varrho+1)}{\Gamma(2\varrho+1)\Gamma(3\varrho+1)} + \Theta_3\vartheta_2 \frac{\Gamma(5\varrho+1)}{\Gamma(3\varrho+1)\Gamma(2\varrho+1)} \\
&\quad + \Theta_4\vartheta_1 \frac{\Gamma(5\varrho+1)}{\Gamma(4\varrho+1)\Gamma(\varrho+1)} + \Theta_5\vartheta_0) - \delta_2(\Theta_0\Psi_5 + \Theta_1\Psi_4 \frac{\Gamma(5\varrho+1)}{\Gamma(\varrho+1)\Gamma(4\varrho+1)} + \\
&\quad \Theta_2\Psi_3 \frac{\Gamma(5\varrho+1)}{\Gamma(2\varrho+1)\Gamma(3\varrho+1)} + \Theta_3\Psi_2 \frac{\Gamma(5\varrho+1)}{\Gamma(3\varrho+1)\Gamma(2\varrho+1)} + \Theta_4\Psi_1 \frac{\Gamma(5\varrho+1)}{\Gamma(4\varrho+1)\Gamma(\varrho+1)} + \Theta_5\Psi_0) - \\
&\quad (\zeta_2 + \omega)\Theta_5, \\
\Psi_6 &= \delta_2(\Theta_0\Psi_5 + \Theta_1\Psi_4 \frac{\Gamma(5\varrho+1)}{\Gamma(\varrho+1)\Gamma(4\varrho+1)} + \Theta_2\Psi_3 \frac{\Gamma(5\varrho+1)}{\Gamma(2\varrho+1)\Gamma(3\varrho+1)} + \Theta_3\Psi_2 \frac{\Gamma(5\varrho+1)}{\Gamma(3\varrho+1)\Gamma(2\varrho+1)} + \\
&\quad \Theta_4\Psi_1 \frac{\Gamma(5\varrho+1)}{\Gamma(4\varrho+1)\Gamma(\varrho+1)} + \Theta_5\Psi_0) + (Y + \zeta_3 + \omega)\Psi_5, \\
\Phi_6 &= Y\Psi_5 - (\theta + \zeta_4 + \omega)\Phi_5, \\
\Omega_6 &= (\beta - \omega)\Omega_5 - (\zeta_1\vartheta_5 + \zeta_2\Theta_5 + \zeta_3\Psi_5 + \zeta_4\Phi_5).
\end{aligned} \tag{20}$$

In this way, we obtained the following 6th-step App-Ss of the Equation (11) in ET space:

$$\vartheta^{*(6)}(\sigma) = \sum_{\nu=0}^6 \vartheta_{\nu} \sigma^{\nu\varrho+2},$$

$$\begin{aligned}
\Theta^{*(6)}(\sigma) &= \sum_{\nu=0}^6 \Theta_{\nu} \sigma^{\nu\varphi+2}, \\
\Psi^{*(6)}(\sigma) &= \sum_{\nu=0}^6 \Psi_{\nu} \sigma^{\nu\varphi+2}, \\
\Phi^{*(6)}(\sigma) &= \sum_{\nu=0}^6 \Phi_{\nu} \sigma^{\nu\varphi+2}, \\
\Omega^{*(6)}(\sigma) &= \sum_{\nu=0}^6 \Omega_{\nu} \sigma^{\nu\varphi+2}.
\end{aligned} \tag{21}$$

We obtained the 6th-step App-Ss of the Equation (2) in real space using the inverse ET as follows:

$$\begin{aligned}
\vartheta^{(6)}(\omega) &= \sum_{\nu=0}^6 \vartheta_{\nu} \frac{\omega^{\nu\varphi+2}}{\Gamma(\nu\varphi+1)}, \\
\Theta^{(6)}(\omega) &= \sum_{\nu=0}^6 \Theta_{\nu} \frac{\omega^{\nu\varphi+2}}{\Gamma(\nu\varphi+1)}, \\
\Psi^{(6)}(\omega) &= \sum_{\nu=0}^6 \Psi_{\nu} \frac{\omega^{\nu\varphi+2}}{\Gamma(\nu\varphi+1)}, \\
\Phi^{(6)}(\omega) &= \sum_{\nu=0}^6 \Phi_{\nu} \frac{\omega^{\nu\varphi+2}}{\Gamma(\nu\varphi+1)}, \\
\Omega^{(6)}(\omega) &= \sum_{\nu=0}^6 \Omega_{\nu} \frac{\omega^{\nu\varphi+2}}{\Gamma(\nu\varphi+1)}.
\end{aligned} \tag{22}$$

To demonstrate the usefulness and efficiency of the ERPSM in handling nonlinear models, we present the numerical results for the App-Ss of the FNLSM presented in Equation (2). Therefore, to obtain the numerical results, utilize the following values of the initial conditions: $\vartheta(0) = 20$, $\Theta(0) = 40$, $\Psi(0) = 60$, $\Phi(0) = 80$, $\Omega(0) = 200$, and parameters: $\beta = 0.1$, $\delta_1 = 0.01$, $\delta_2 = 0.001$, $\zeta_1 = 0.33$, $\zeta_2 = 0.44$, $\zeta_3 = 0.55$, $\zeta_4 = 0.66$, $\theta = 0.2$, $\omega = 0.05$, $Y = 0.99$ [25], we have the following coefficients of FPS.

By utilizing the initial conditions and parameter values in Equations (15) and (16), we obtain the 1st and 2nd coefficients of FPS as follows: $\vartheta_1 = 20.4$, $\Theta_1 = -14$, $\Psi_1 = -93$, $\Phi_1 = -13.4$, $\Omega_1 = -100$. $\vartheta_2 = -25.792$, $\Theta_2 = 16.78$, $\Psi_2 = 143.31$, $\Phi_2 = -79.876$, $\Omega_2 = 54.422$. By using the initial conditions and parameter values in Equation (17) we obtain the 3rd coefficient of FPS as follows:

$$\begin{aligned}
\vartheta_3 &= \frac{2.856\Gamma(2\varphi+1)}{\Gamma(\varphi+1)^2} + 6.22876, \\
\Theta_3 &= -\frac{4.158\Gamma(2\varphi+1)}{\Gamma(\varphi+1)^2} - 21.9222, \\
\Psi_3 &= \frac{1.302\Gamma(2\varphi+1)}{\Gamma(\varphi+1)^2} - 221.124, \\
\Phi_3 &= 214.564, \\
\Omega_3 &= -22.2531.
\end{aligned} \tag{23}$$

In the same way, by utilizing the same initial conditions and parameter values in Equation (18), we obtain the 4th coefficient of FPS as follows:

$$\begin{aligned}
\vartheta_4 &= -\frac{1.39608\Gamma(2\varphi+1)}{\Gamma(\varphi+1)^2} - \frac{7.034\Gamma(3\varphi+1)}{\Gamma(\varphi+1)\Gamma(2\varphi+1)} + 40.2135, \\
\Theta_4 &= \frac{0.5082\Gamma(2\varphi+1)}{\Gamma(\varphi+1)^2} + \frac{10.6009\Gamma(3\varphi+1)}{\Gamma(\varphi+1)\Gamma(2\varphi+1)} + 8.26734,
\end{aligned}$$

$$\begin{aligned}\Psi_4 &= -\frac{2.26758\Gamma(2\varphi+1)}{\Gamma(\varphi+1)^2} - \frac{3.56688\Gamma(3\varphi+1)}{\Gamma(\varphi+1)\Gamma(2\varphi+1)} + 341.426, \\ \Phi_4 &= \frac{1.28898\Gamma(2\varphi+1)}{\Gamma(\varphi+1)^2} - 414.166, \\ \Omega_4 &= \frac{0.17094\Gamma(2\varphi+1)}{\Gamma(\varphi+1)^2} - 13.5166.\end{aligned}\quad (24)$$

In the same manner, by utilizing the same values in Equations (19) and (20), we obtain the 5th and 6th coefficients of FPS as follows:

$$\begin{aligned}\vartheta_5 &= \frac{1.24807\Gamma(4\varphi+1)\Gamma(2\varphi+1)}{\Gamma(\varphi+1)^3\Gamma(3\varphi+1)} + \frac{1.26219\Gamma(2\varphi+1)}{\Gamma(\varphi+1)^2} + \frac{\frac{3.36634\Gamma(3\varphi+1)}{\Gamma(2\varphi+1)} + \frac{5.34416\Gamma(4\varphi+1)}{\Gamma(3\varphi+1)}}{\Gamma(\varphi+1)} + \\ &\quad \frac{4.3279\Gamma(4\varphi+1)}{\Gamma(2\varphi+1)^2} - 117.205, \\ \Theta_5 &= \frac{0.368466\Gamma(4\varphi+1)\Gamma(2\varphi+1)}{\Gamma(\varphi+1)^3\Gamma(3\varphi+1)} + \frac{3.54524\Gamma(2\varphi+1)}{\Gamma(\varphi+1)^2} + \frac{\frac{6.16472\Gamma(3\varphi+1)}{\Gamma(2\varphi+1)} + \frac{5.1345\Gamma(4\varphi+1)}{\Gamma(3\varphi+1)}}{\Gamma(\varphi+1)} + \\ &\quad \frac{2.40474\Gamma(4\varphi+1)}{\Gamma(2\varphi+1)^2} - 528.715, \\ \Psi_5 &= -\frac{3.41788\Gamma(2\varphi+1)}{\Gamma(\varphi+1)^2} - \frac{3.53121\Gamma(3\varphi+1)}{\Gamma(\varphi+1)\Gamma(2\varphi+1)} + 714.903, \\ \Phi_5 &= -\frac{3.41788\Gamma(2\varphi+1)}{\Gamma(\varphi+1)^2} - \frac{3.53121\Gamma(3\varphi+1)}{\Gamma(\varphi+1)\Gamma(2\varphi+1)} + 714.903, \\ \Omega_5 &= \frac{0.642088\Gamma(2\varphi+1)}{\Gamma(\varphi+1)^2} - \frac{0.381383\Gamma(3\varphi+1)}{\Gamma(\varphi+1)\Gamma(2\varphi+1)} + 67.981. \\ \vartheta_6 &= \frac{-\frac{3.13277\Gamma(3\varphi+1)}{\Gamma(2\varphi+1)} + \frac{3.94335\Gamma(5\varphi+1)}{\Gamma(4\varphi+1)} - \frac{2.07271\Gamma(4\varphi+1)}{\Gamma(3\varphi+1)}}{\Gamma(\varphi+1)} + \\ &\quad \frac{-1.52456\Gamma(2\varphi+1) - \frac{1.55167\Gamma(5\varphi+1)}{\Gamma(3\varphi+1)} - \frac{3.14734\Gamma(3\varphi+1)\Gamma(5\varphi+1)}{\Gamma(2\varphi+1)\Gamma(4\varphi+1)}}{\Gamma(\varphi+1)^2} + \\ &\quad \frac{\Gamma(2\varphi+1)\left(-\frac{0.650189\Gamma(4\varphi+1)^2}{\Gamma(3\varphi+1)} - 0.299124\Gamma(5\varphi+1)\right)}{\Gamma(\varphi+1)^3\Gamma(4\varphi+1)} - \frac{2.02923\Gamma(4\varphi+1)}{\Gamma(2\varphi+1)^2} - \\ &\quad \frac{6.69936\Gamma(5\varphi+1)}{\Gamma(2\varphi+1)\Gamma(3\varphi+1)} + 240.481, \\ \Theta_6 &= \frac{\frac{0.933797\Gamma(3\varphi+1)}{\Gamma(2\varphi+1)} + \frac{1.60548\Gamma(5\varphi+1)}{\Gamma(4\varphi+1)} + \frac{0.465271\Gamma(4\varphi+1)}{\Gamma(3\varphi+1)}}{\Gamma(\varphi+1)} + \frac{0.6924\Gamma(4\varphi+1)}{\Gamma(2\varphi+1)^2} + \\ &\quad \frac{0.307546\Gamma(2\varphi+1) + \frac{2.1257\Gamma(5\varphi+1)}{\Gamma(3\varphi+1)} + \frac{4.08329\Gamma(3\varphi+1)\Gamma(5\varphi+1)}{\Gamma(2\varphi+1)\Gamma(4\varphi+1)}}{\Gamma(\varphi+1)^2} + \\ &\quad \frac{\Gamma(2\varphi+1)\left(\frac{0.258175\Gamma(4\varphi+1)^2}{\Gamma(3\varphi+1)} + 0.31464\Gamma(5\varphi+1)\right)}{\Gamma(\varphi+1)^3\Gamma(4\varphi+1)} + \frac{13.5515\Gamma(5\varphi+1)}{\Gamma(2\varphi+1)\Gamma(3\varphi+1)} - 25.2313, \\ \Psi_6 &= \frac{-\frac{9.62652\Gamma(3\varphi+1)}{\Gamma(2\varphi+1)} - \frac{5.54883\Gamma(5\varphi+1)}{\Gamma(4\varphi+1)} - \frac{8.58719\Gamma(4\varphi+1)}{\Gamma(3\varphi+1)}}{\Gamma(\varphi+1)} + \\ &\quad \frac{-5.51892\Gamma(2\varphi+1) - \frac{0.574035\Gamma(5\varphi+1)}{\Gamma(3\varphi+1)} - \frac{0.935946\Gamma(3\varphi+1)\Gamma(5\varphi+1)}{\Gamma(2\varphi+1)\Gamma(4\varphi+1)}}{\Gamma(\varphi+1)^2} + \\ &\quad \frac{\Gamma(2\varphi+1)\left(-\frac{0.668115\Gamma(4\varphi+1)^2}{\Gamma(3\varphi+1)} - 0.0155165\Gamma(5\varphi+1)\right)}{\Gamma(\varphi+1)^3\Gamma(4\varphi+1)} - \frac{4.13131\Gamma(4\varphi+1)}{\Gamma(2\varphi+1)^2}\end{aligned}\quad (25)$$

$$\begin{aligned}
& - \frac{6.85213\Gamma(5\varphi + 1)}{\Gamma(2\varphi + 1)\Gamma(3\varphi + 1)} + 819.723, \\
\Phi_6 = & \frac{0.364781\Gamma(4\varphi + 1)\Gamma(2\varphi + 1)}{\Gamma(\varphi + 1)^3\Gamma(3\varphi + 1)} + \frac{6.62006\Gamma(2\varphi + 1)}{\Gamma(\varphi + 1)^2} + \frac{9.31647\Gamma(3\varphi + 1)}{\Gamma(2\varphi + 1)} + \frac{5.08315\Gamma(4\varphi + 1)}{\Gamma(3\varphi + 1)} + \\
& \frac{2.38069\Gamma(4\varphi + 1)}{\Gamma(2\varphi + 1)^2} - 1173.99, \\
\Omega_6 = & \frac{0.0967567\Gamma(4\varphi + 1)\Gamma(2\varphi + 1)}{\Gamma(\varphi + 1)^3\Gamma(3\varphi + 1)} + \frac{0.095992\Gamma(2\varphi + 1)}{\Gamma(\varphi + 1)^2} + \frac{0.0230625\Gamma(4\varphi + 1)}{\Gamma(3\varphi + 1)} - \frac{1.66776\Gamma(3\varphi + 1)}{\Gamma(2\varphi + 1)} \\
& + \frac{0.211547\Gamma(4\varphi + 1)}{\Gamma(2\varphi + 1)^2} - 140.544.
\end{aligned} \tag{26}$$

The 6th-step App-Ss produced by ERPSM in terms of $\vartheta(\omega)$, $\Theta(\omega)$, $\Psi(\omega)$, $\Phi(\omega)$, and $\Omega(\omega)$ at $\varphi = 0.6, 0.7, 0.8, 0.9$, and 1.0 are shown below.

By utilizing the numerical values of the coefficients of FPS in Equation (22), we obtain 6th-step App-Ss of $\vartheta(\omega)$ at $\varphi = 0.6, 0.7, 0.8, 0.9$, and 1.0 , respectively, as follows:

$$\begin{aligned}
\vartheta^6(\omega) = & 20 + 22.8312\omega^{0.6} - 23.4089\omega^{1.2} + 6.06638\omega^{1.8} + 8.82477\omega^{2.4} - 14.1731\omega^{3.0} + 14.1475\omega^{3.6}, \\
\vartheta^6(\omega) = & 20 + 22.4512\omega^{0.7} - 20.7637\omega^{1.4} + 4.78958\omega^{2.1} + 5.20164\omega^{2.8} - 6.75802\omega^{3.5} + 5.31228\omega^{4.2}, \\
\vartheta^6(\omega) = & 20 + 21.9029\omega^{0.8} - 18.0411\omega^{1.6} + 3.66816\omega^{2.4} + 2.85741\omega^{3.2} - 2.93698\omega^{4.0} + 1.75654\omega^{4.8}, \\
\vartheta^6(\omega) = & 20 + 21.211\omega^{0.9} - 15.3845\omega^{1.8} + 2.7346\omega^{2.7} + 1.45643\omega^{3.6} - 1.15069\omega^{4.5} + 0.492564\omega^{5.4}, \\
\vartheta^6(\omega) = & 20 + 20.4\omega^{1.0} - 12.896\omega^{2.0} + 1.99013\omega^{3.0} + 0.679973\omega^{4.0} - 0.393774\omega^{5.0} + 0.102576\omega^{6.0}.
\end{aligned} \tag{27}$$

By utilizing the numerical values of the coefficients of FPS in Equation (22), we obtain 6th-step App-Ss of $\Theta(\omega)$ at $\varphi = 0.6, 0.7, 0.8, 0.9$, and 1.0 respectively, as follows:

$$\begin{aligned}
\Theta^6(\omega) = & 40 - 15.6684\omega^{0.6} + 15.2296\omega^{1.2} - 16.4991\omega^{1.8} + 9.06384\omega^{2.4} - 6.80173\omega^{3.0} + 4.02973\omega^{3.6}, \\
\Theta^6(\omega) = & 40 - 15.4077\omega^{0.7} + 13.5086\omega^{1.4} - 12.8221\omega^{2.1} + 6.32114\omega^{2.8} - 4.31189\omega^{3.5} + 2.45206\omega^{4.2}, \\
\Theta^6(\omega) = & 40 - 15.0314\omega^{0.8} + 11.7373\omega^{1.6} - 9.65203\omega^{2.4} + 4.23371\omega^{3.2} - 2.58298\omega^{4.0} + 1.35418\omega^{4.8}, \\
\Theta^6(\omega) = & 40 - 14.5566\omega^{0.9} + 10.009\omega^{1.8} - 7.06324\omega^{2.7} + 2.73583\omega^{3.6} - 1.47083\omega^{4.5} + 0.690291\omega^{5.4}, \\
\Theta^6(\omega) = & 40 - 14\omega^{1.0} + 8.39\omega^{2.0} - 5.0397\omega^{3.0} + 1.71193\omega^{4.0} - 0.800088\omega^{5.0} + 0.328775\omega^{6.0}.
\end{aligned} \tag{28}$$

By utilizing the numerical values of the coefficients of FPS in Equation (22), we obtain 6th-step App-Ss of $\Psi(\omega)$ at $\varphi = 0.6, 0.7, 0.8, 0.9$, and 1.0 respectively, as follows:

$$\begin{aligned}
\Psi^6(\omega) = & 60 - 104.083\omega^{0.6} + 130.069\omega^{1.2} - 130.825\omega^{1.8} + 111.439\omega^{2.4} - 82.698\omega^{3.0} + 54.2306\omega^{3.6}, \\
\Psi^6(\omega) = & 60 - 102.351\omega^{0.7} + 115.371\omega^{1.4} - 99.7282\omega^{2.1} + 70.5278\omega^{2.8} - 42.1854\omega^{3.5} + 21.6255\omega^{4.2}, \\
\Psi^6(\omega) = & 60 - 99.8514\omega^{0.8} + 100.243\omega^{1.6} - 73.4528\omega^{2.4} + 42.5057\omega^{3.2} - 20.1626\omega^{4.0} + 7.90615\omega^{4.8}, \\
\Psi^6(\omega) = & 60 - 96.6971\omega^{0.9} + 85.4821\omega^{1.8} - 52.4532\omega^{2.7} + 24.5186\omega^{3.6} - 9.08508\omega^{4.5} + 2.66097\omega^{5.4}, \\
\Psi^6(\omega) = & 60 - 93\omega^{1.0} + 71.655\omega^{2.0} - 36.42\omega^{3.0} + 13.5913\omega^{4.0} - 3.8768\omega^{5.0} + 0.824144\omega^{6.0}.
\end{aligned} \tag{29}$$

By utilizing the numerical values of the coefficients of FPS in Equation (22), we obtain 6th-step App-Ss of $\Phi(\omega)$ at $\varphi = 0.6, 0.7, 0.8, 0.9$, and 1.0 respectively, as follows:

$$\begin{aligned}
\Phi^6(\omega) = & 80 - 14.9969\omega^{0.6} - 72.4958\omega^{1.2} + 127.984\omega^{1.8} - 138.329\omega^{2.4} + 117.362\omega^{3.0} - 84.5975\omega^{3.6}, \\
\Phi^6(\omega) = & 80 - 14.7473\omega^{0.7} - 64.3036\omega^{1.4} + 97.6347\omega^{2.1} - 87.8166\omega^{2.8} + 60.4283\omega^{3.5} - 34.5449\omega^{4.2}, \\
\Phi^6(\omega) = & 80 - 14.3872\omega^{0.8} - 55.872\omega^{1.6} + 71.9722\omega^{2.4} - 53.1208\omega^{3.2} + 29.2235\omega^{4.0} - 13.0493\omega^{4.8}, \\
\Phi^6(\omega) = & 80 - 13.9327\omega^{0.9} - 47.6448\omega^{1.8} + 51.4462\omega^{2.7} - 30.7765\omega^{3.6} + 13.3653\omega^{4.5} - 4.59817\omega^{5.4}, \\
\Phi^6(\omega) = & 80 - 13.4\omega^{1.0} - 39.938\omega^{2.0} + 35.7607\omega^{3.0} - 17.1495\omega^{4.0} + 5.81228\omega^{5.0} - 1.5212\omega^{6.0}.
\end{aligned} \tag{30}$$

By utilizing the numerical values of the coefficients of FPS in Equation (22), we obtain 6th-step App-Ss of $\Omega(\omega)$ at $\varphi = 0.6, 0.7, 0.8, 0.9,$ and 1.0 respectively, as follows:

$$\begin{aligned}\Omega^6(\omega) &= 200 - 111.917\omega^{0.6} + 49.3936\omega^{1.2} - 13.2736\omega^{1.8} - 4.45481\omega^{2.4} + 11.3696\omega^{3.0} - 10.6432\omega^{3.6}, \\ \Omega^6(\omega) &= 200 - 110.055\omega^{0.7} + 43.8121\omega^{1.4} - 10.126\omega^{2.1} - 2.82466\omega^{2.8} + 5.86365\omega^{3.5} - 4.37738\omega^{4.2}, \\ \Omega^6(\omega) &= 200 - 107.367\omega^{0.8} + 38.0673\omega^{1.6} - 7.46445\omega^{2.4} - 1.70626\omega^{3.2} + 2.84105\omega^{4.0} - 1.66788\omega^{4.8}, \\ \Omega^6(\omega) &= 200 - 103.975\omega^{0.9} + 32.4619\omega^{1.8} - 5.33564\omega^{2.7} - 0.986961\omega^{3.6} + 1.30215\omega^{4.5} - 0.593831\omega^{5.4}, \\ \Omega^6(\omega) &= 200 - 100\omega^{1.0} + 27.211\omega^{2.0} - 3.70885\omega^{3.0} - 0.548948\omega^{4.0} + 0.567675\omega^{5.0} - 0.198916\omega^{6.0}.\end{aligned}\quad (31)$$

Based on their graphical and numerical outcomes, the approximations established by the ERPSM for the FNLSM are reviewed and evaluated in the next section.

4. Graphical and Numerical Results of Approximate Solutions Attained by ERPSM

In this section, we evaluate the graphical and numerical results of the approximate solutions for the five groups of smokers discussed in Section 3. Error functions are utilized to assess the precision and capabilities of the approximation method. Since ERPSM provides an approximate solution in terms of an infinite FPS, it is necessary to indicate the errors of the approximate solution. To illustrate the precision and capability of ERPSM, we employ the recurrence and residual error functions.

Figures 1–3 illustrate the behaviors of the 6th-step App-Ss derived by ERPSM for potential smokers $\vartheta(\omega)$, light smokers $\Theta(\omega)$, smokers $\Psi(\omega)$, quit smokers $\Phi(\omega)$, and total smokers $\Omega(\omega)$ for various fractional derivative values, including $\varphi = 0.6, 0.7, 0.8, 0.9,$ and 1.0 , within the interval $\omega \in [0, 2.0]$. From these figures, it is evident that the FNLSM exhibits a higher degree of freedom due to the utilization of fractional derivatives. The results show that the decline is significant for the lower fractional order but not as much for the higher order. It is important to note that we used a short period of time because we considered small initial values. The initial data should be sufficiently large for a longer time interval. Moreover, from these figures, we concluded that ERPSM yielded results that are in accordance with [25], which established the reliability and effectiveness of the suggested method for solving fractional nonlinear problems that arise in biological systems. Figures 4–6 are used to assess the accuracy of the proposed method. These figures depict the Res-Errors obtained by the ERPSM for the FNLSM's 6th-step App-Ss in the range $\omega \in [0, 0.5]$. For all sorts of smokers, we observed that the Res-Errors are incredibly small. We come to the conclusion that the proposed method provides a very accurate App-Ss in the form of a series. The convergence of the App-Ss to the exact solutions for FNLSM has been illustrated graphically using Rec-Errors in the interval $\omega \in [0, 0.5]$ at $\varphi = 1.0$, as shown in Figures 7–11. These figures demonstrate that the suggested method quickly converges to the exact solutions because the Rec-Errors for the 5th-step App-Ss are very small, but they get even smaller for the 6th-step App-Ss. The Rec-Errors study confirmed the high level of convergence rates of App-Ss achieved by ERPSM. We therefore came to the conclusion that the proposed method is a practical and effective technique for solving nonlinear fractional models.

Tables 1–5 show how the 6th-step App-Ss of $\vartheta(\omega)$, $\Theta(\omega)$, $\Psi(\omega)$, $\Phi(\omega)$ and $\Omega(\omega)$ obtained by ERPSM behave at different $\varphi = 0.5, 0.6, 0.7, 0.8, 0.9,$ and 1.0 FD values in the $\omega \in [0, 1.0]$ interval. Tables 6 and 7 show the Res-Errors for the 5th and 6th apps in the interval $\omega \in [0, 0.5]$ as obtained by the ERPSM for the FNLSM at $\varphi = 1.0$. From these tables, we observed that the Res-Errors for all the kinds of smokers in the 5th step App-Ss are very small. When we consider 6th-step App-Ss for all categories of smokers, the Rec-Errors become even smaller. This process of Rec-Errors shows the accuracy of our proposed method, and hence the approximation is rapidly converging to the exact solution. Tables 8 and 9 compare the Res-errors of the third-step App-Ss derived by ERPSM and LDM [24] for all types of smokers in the $\omega \in [0, 0.5]$ range. The results obtained using the proposed method show clear agreement with the LDM, confirming that the

ERPSM is a useful substitute method in the solution of fractional nonlinear problems in biological systems.

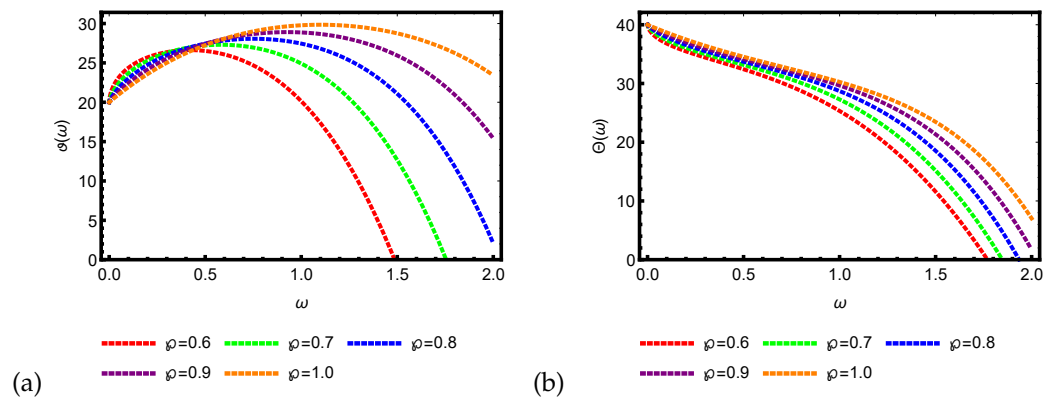


Figure 1. The behavior of 6th-step App-Ss with $\varrho = 0.6, 0.7, 0.8, 0.9, 1.0$ of (a) potential smokers, $\vartheta(\omega)$; (b) light smokers, $\Theta(\omega)$.

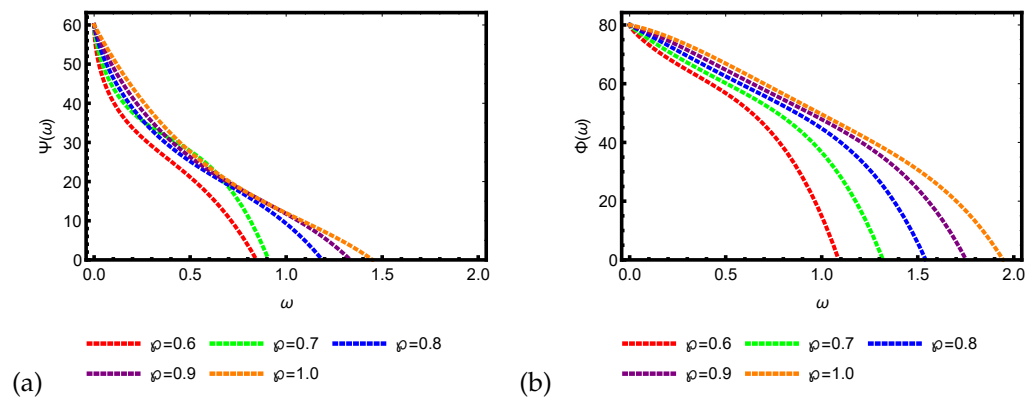


Figure 2. The behavior of 6th-step App-Ss with $\varrho = 0.6, 0.7, 0.8, 0.9, 1.0$ of (a) smokers, $\Psi(\omega)$; (b) quit smokers, $\Phi(\omega)$.

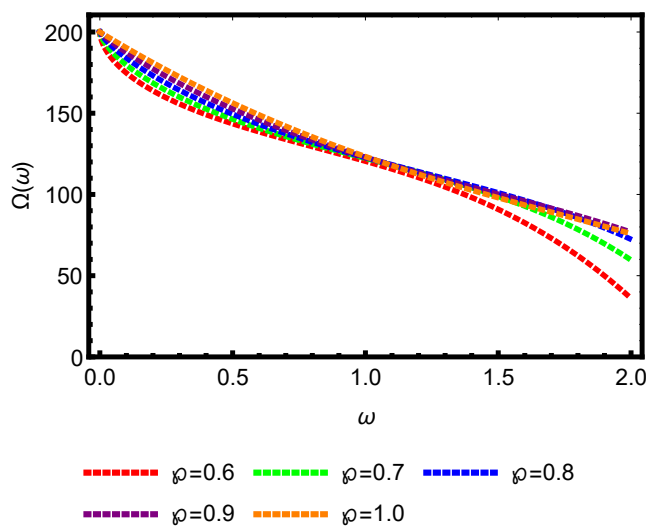


Figure 3. The behavior of 6th-step App-S with $\varrho = 0.6, 0.7, 0.8, 0.9, 1.0$ of total smokers, $\Omega(\omega)$.

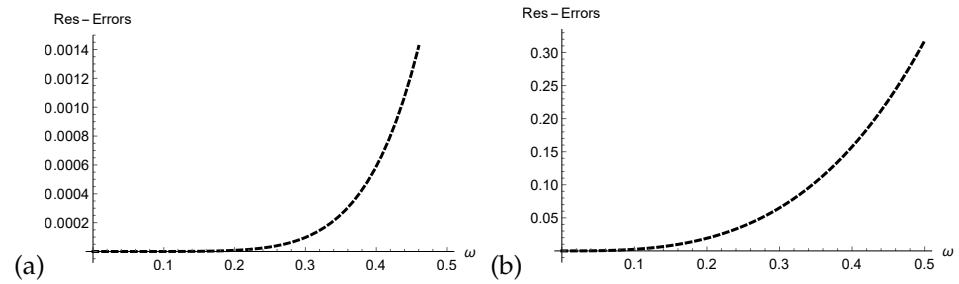


Figure 4. The Res-Errors of 6th-step App-Ss are as follows: (a) potential smokers, $\vartheta(\omega)$; (b) light smokers, $\Theta(\omega)$ at $\varphi = 1.0$.

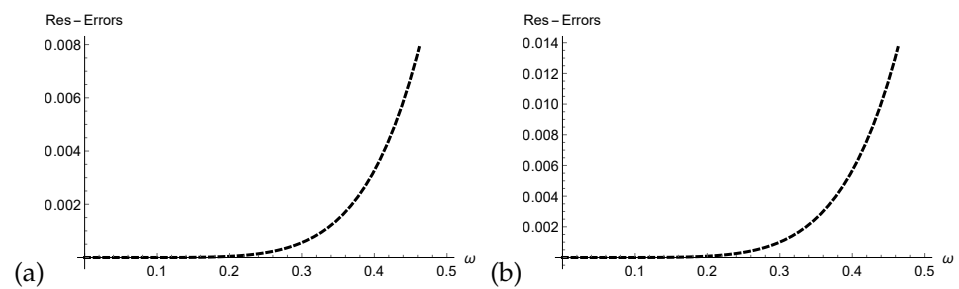


Figure 5. The Res-Errors of 6th-step App-Ss are as follows: (a) smokers, $\Psi(\omega)$; (b) quit smokers, $\Phi(\omega)$ at $\varphi = 1.0$.

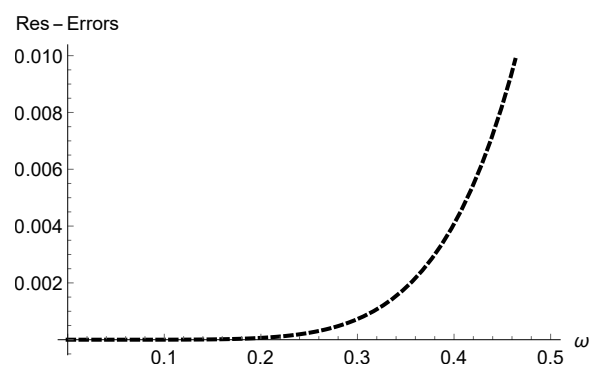


Figure 6. The Res-Errors of 6th-step App-S for total smokers $\Omega(\omega)$.

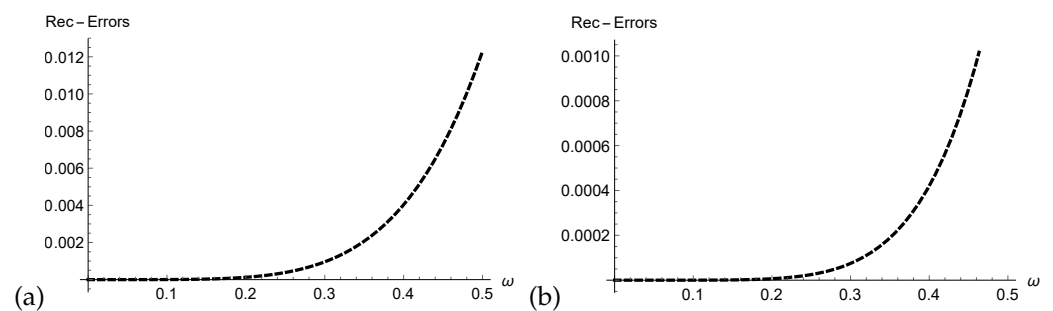


Figure 7. Graphs of Rec-Errors in the interval $\omega \in [0, 0.5]$ when $\varphi = 1.0$: (a) $|\vartheta^5(\omega) - \vartheta^4(\omega)|$, (b) $|\vartheta^6(\omega) - \vartheta^5(\omega)|$.

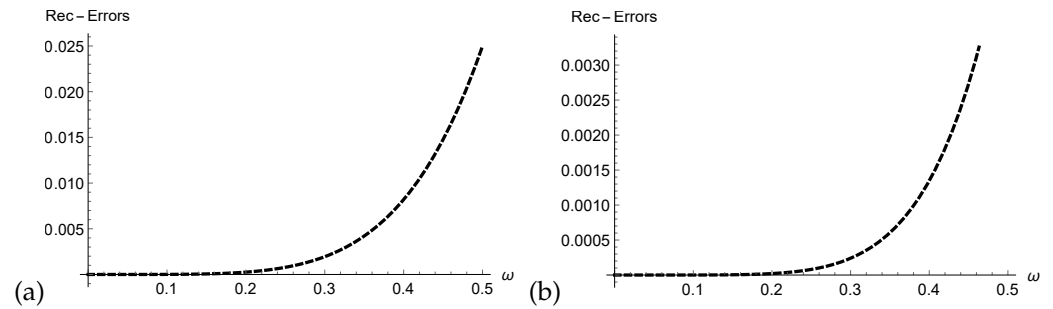


Figure 8. Graphs of Rec-Errors in the interval $\omega \in [0, 0.5]$ when $\varphi = 1.0$: (a) $|\Theta^5(\omega) - \Theta^4(\omega)|$, (b) $|\Theta^6(\omega) - \Theta^5(\omega)|$.

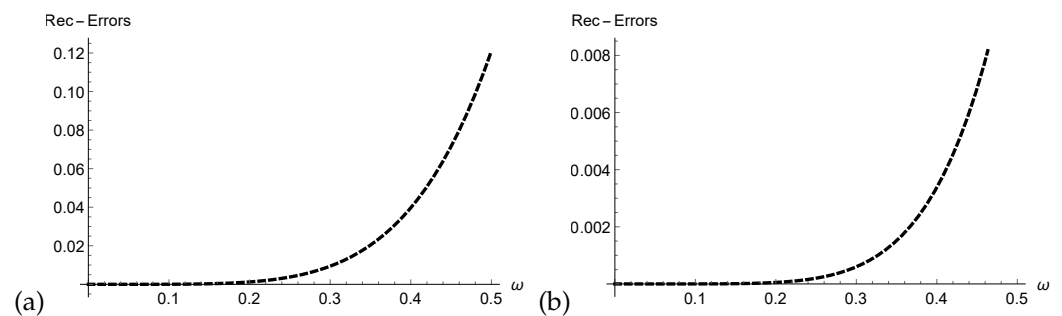


Figure 9. Graphs of Rec-Errors in the interval $\omega \in [0, 0.5]$ when $\varphi = 1.0$: (a) $|\Psi^5(\omega) - \Psi^4(\omega)|$, (b) $|\Psi^6(\omega) - \Psi^5(\omega)|$.

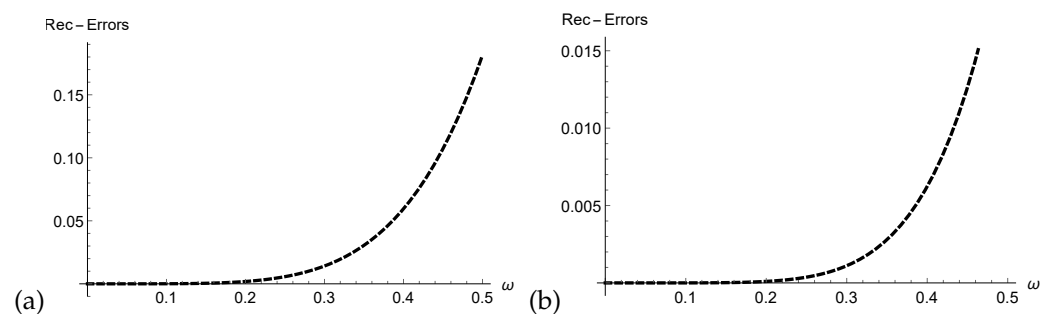


Figure 10. Graphs of Rec-Errors in the interval $\omega \in [0, 0.5]$ when $\varphi = 1.0$: (a) $|\Phi^5(\omega) - \Phi^4(\omega)|$, (b) $|\Phi^6(\omega) - \Phi^5(\omega)|$.

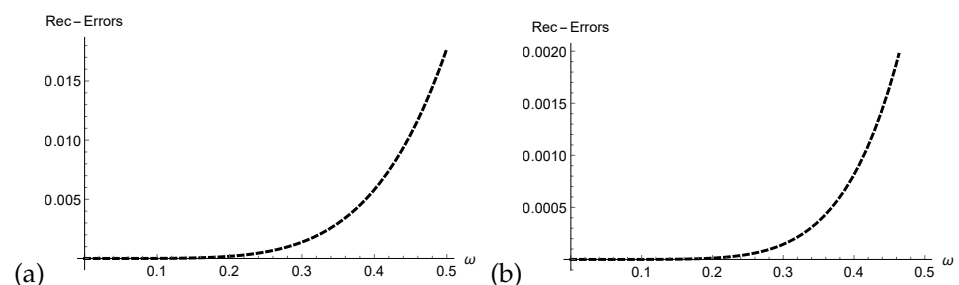


Figure 11. Graphs of Rec-Errors in the interval $\omega \in [0, 0.5]$ when $\varphi = 1.0$: (a) $|\Omega^5(\omega) - \Omega^4(\omega)|$, (b) $|\Omega^6(\omega) - \Omega^5(\omega)|$.

In the following tables, we conduct a comparative study of our results obtained by ERPSM with those obtained by LDM [24] in the framework of Res-Errors. We observe that the results obtained by both methods are highly consistent with each other. Therefore, we conclude that ERPSM is an alternative method for solving NFDES in a straightforward manner.

Table 1. $\vartheta(\omega)$ behavior at various \wp values.

ω	$\wp = 0.6$	$\wp = 0.7$	$\wp = 0.8$	$\wp = 0.9$	$\wp = 1.0$
0.1	24.3750	23.6971	23.0343	28.8668	21.9131
0.2	25.7061	25.2921	24.7592	28.8668	23.581
0.3	26.3695	26.2781	25.9725	28.8668	25.0176
0.4	26.6172	26.8904	26.8427	28.8668	26.2374
0.5	26.5161	27.2191	27.4509	28.8668	27.2551
0.6	26.0702	27.2979	27.8413	28.8668	28.0848
0.7	25.2547	27.1300	28.0358	28.8668	28.7407
0.8	24.0291	26.6996	28.0411	28.8668	29.235
0.9	22.3432	25.9767	27.8513	28.8668	29.5787
1.0	20.1403	24.9207	27.4504	28.8668	29.7803

Table 2. $\Theta(\omega)$ behavior at various \wp values.

ω	$\wp = 0.6$	$\wp = 0.7$	$\wp = 0.8$	$\wp = 0.9$	$\wp = 1.0$
0.1	36.7931	37.3704	37.8765	38.3126	38.6792
0.2	35.4676	36.0428	36.5635	37.0484	37.4978
0.3	34.4138	35.0008	35.505	35.976	36.4312
0.4	33.4292	34.0719	34.5765	35.0243	35.4555
0.5	32.4207	33.1699	33.7091	34.1473	34.5495
0.6	31.3302	32.2363	32.8527	33.3081	33.6915
0.7	30.1124	31.2237	31.9646	32.4733	32.8593
0.8	28.7286	30.089	31.0045	31.6097	32.0283
0.9	27.1437	28.7909	29.9319	30.6825	31.1727
1.0	25.3242	27.2881	28.7046	29.6542	30.2621

Table 3. $\Psi(\omega)$ behavior at various \wp values.

ω	$\wp = 0.6$	$\wp = 0.7$	$\wp = 0.8$	$\wp = 0.9$	$\wp = 1.0$
0.1	40.3498	43.4776	46.4251	49.0826	51.3815
0.2	33.6865	36.1773	38.7503	41.3893	43.9953
0.3	31.3447	31.1612	33.1467	35.3161	37.6663
0.4	25.1759	27.2493	28.7682	30.3769	32.2422
0.5	21.1535	23.8488	25.1668	26.2779	27.5896
0.6	16.5328	20.5494	22.0337	22.8044	23.5891
0.7	10.884	17.0038	19.1155	19.7788	20.1306
0.8	3.81331	12.8878	16.1771	17.0388	17.1088
0.9	0.0000	7.87628	12.9823	14.4238	14.4184
1.0	0.0000	1.6342	9.28190	11.7653	11.9495

Table 4. $\Phi(\omega)$ behavior at various \wp values.

ω	$\wp = 0.6$	$\wp = 0.7$	$\wp = 0.8$	$\wp = 0.9$	$\wp = 1.0$
0.1	73.2326	75.1508	76.5721	77.5862	78.2947
0.2	68.6195	70.9958	73.0208	74.6795	75.9829
0.3	64.6459	67.1806	69.4402	71.4721	73.2252
0.4	60.8445	63.6189	65.9297	68.1171	70.1529
0.5	56.7892	60.1818	62.5195	64.7121	66.8716
0.6	52.0247	56.6919	59.1907	61.3152	63.465
0.7	46.0478	52.9183	55.8813	57.9519	59.9966
0.8	38.2974	48.5693	52.4854	54.6175	56.5105
0.9	28.1516	43.2892	48.8494	51.2765	53.0316
1.0	14.9268	36.6506	44.7664	47.8593	50.0316

Table 5. $\Omega(\omega)$ behavior at various \wp values.

ω	$\wp = 0.6$	$\wp = 0.7$	$\wp = 0.8$	$\wp = 0.9$	$\wp = 1.0$
0.1	174.7853	179.7025	183.9093	187.4144	190.2682
0.2	163.7824	168.5715	173.1086	177.2942	181.0585
0.3	155.7041	159.8945	164.13322	168.3195	172.3465
0.4	149.1545	152.6465	156.3363	160.1892	164.1075
0.5	143.5553	146.3673	149.4094	152.7442	156.3195
0.6	138.5483	140.7923	143.1632	145.8825	148.9592
0.7	133.9145	135.7273	137.4642	139.5225	142.0012
0.8	129.4625	131.0385	132.2115	133.6035	135.4255
0.9	125.0315	126.5975	127.3175	128.0733	129.2065
1.0	121.0312	122.5973	123.3175	122.0735	139.2463

Table 6. The Rec-Errors for the App-Ss in the 5th and 6th iterations for $\vartheta(\omega)$, $\Theta(\omega)$, and $\Psi(\omega)$.

ω	Rec-Errors	Rec-Errors	Rec-Errors	Rec-Errors	Rec-Errors	Rec-Errors
	$ \vartheta^{(5)} - \vartheta^{(4)} $	$ \vartheta^{(6)} - \vartheta^{(5)} $	$ \Theta^{(5)} - \Theta^{(4)} $	$ \Theta^{(6)} - \Theta^{(5)} $	$ \Psi^{(5)} - \Psi^{(4)} $	$ \Psi^{(6)} - \Psi^{(5)} $
0.1	0.00000393774	0.00000010258	0.00000800088	0.00000032878	0.00003876801	0.00000082414
0.2	0.00012600801	0.00000656485	0.00025602801	0.00002104160	0.00124058012	0.00005274521
0.3	0.00095687100	0.00007477780	0.00194421001	0.00023967701	0.00942063101	0.00060080102
0.4	0.00403225001	0.00042015101	0.00819290001	0.00134666021	0.03969840102	0.00337569001
0.5	0.01230540120	0.00160275001	0.02500270012	0.00513711011	0.12115110001	0.01287730011

Table 7. The Rec-Errors for the App-Ss in the 5th and 6th iterations for $\Phi(\omega)$ and $\Omega(\omega)$.

ω	Rec-Errors	Rec-Errors	Rec-Errors	Rec-Errors
	$ \Phi^{(5)} - \Phi^{(4)} $	$ \Phi^{(6)} - \Phi^{(5)} $	$ \Omega^{(5)} - \Omega^{(4)} $	$ \Omega^{(6)} - \Omega^{(5)} $
0.1	0.00005812280	0.000001521201	0.00000567675	0.00000019891
0.2	0.00185993010	0.000097356900	0.00018165601	0.00001273060
0.3	0.01412380001	0.00110896002	0.00137945001	0.00014501001
0.4	0.05951770003	0.006230840010	0.00581299002	0.00081476002
0.5	0.18163410201	0.02376880001	0.01773981020	0.00310806003

Table 8. The comparison of Res-Errors in 3rd-step App-Ss of $\vartheta(\omega)$, $\Theta(\omega)$, and $\Psi(\omega)$ obtained by ERPSM and SDM.

ω	Res-Errors	Res-Errors	Res-Errors	Res-Errors	Res-Errors	Res-Errors
	$[\vartheta(\omega)][ERPSM]$	$[\vartheta(\omega)][LDM]$	$[\Theta(\omega)][ERPSM]$	$[\Theta(\omega)][LDM]$	$[\Psi(\omega)][ERPSM]$	$[\Psi(\omega)][LDM]$
0.1	0.00295059101	0.00295059101	0.00896119120	0.00896119120	0.00797612010	0.00797612010
0.2	0.02532571201	0.02532571201	0.06905251122	0.06905251122	0.00440025120	0.00440025120
0.3	0.09087270012	0.09087270012	0.224824110011	0.224824110011	0.00055981812	0.00055981812
0.4	0.22726811220	0.22726811220	0.51490300001	0.51490300001	0.00326328012	0.00326328012
0.5	0.46531721210	0.46531721210	0.97319521210	0.97319521210	0.01277340001	0.01277340001

Table 9. The comparison of Res-Errors in 3rd-step App-Ss of $\Phi(\omega)$ and $\Omega(\omega)$ obtained by ERPSM and SDM.

ω	Res-Errors	Res-Errors	Res-Errors	Res-Errors
	$[\Phi(\omega)][ERPSM]$	$[\Phi(\omega)][LDM]$	$[\Omega(\omega)][ERPSM]$	$[\Omega(\omega)][LDM]$
0.1	0.00290541001	0.00290541001	0.00028394910	0.00028394910
0.2	0.00464952002	0.00464952002	0.00454189120	0.00454189120
0.3	0.02353910210	0.02353910210	0.02299221120	0.02299221120
0.4	0.07439590211	0.07439590211	0.07266461101	0.07266461101
0.5	0.81632002110	0.81632002110	0.17740211210	0.17740211210

5. Conclusions

In this research, we have utilized a novel straightforward approximate technique known as ERPSM to establish approximate series and numerical solutions for the FNLSM, which has held significant importance in applied sciences. The precision and convergence rates have been demonstrated through Res-Errors and Rec-Errors analyses, presented both graphically and numerically. ERPSM has proven to be a valuable alternative tool for solving fractional nonlinear models in biological systems, as evidenced by the outcomes demonstrating strong alignment with the LDM.

The advantages of ERPSM over other methods for providing approximate solutions, as evidenced by the results, can be summarized as follows: ERPSM determines the coefficients of terms of the series solution by applying the straightforward limit principle at zero. In contrast, other established methods like VIM, ADM, and HPM have necessitated integration, while RPSM has relied on derivatives, both of which have posed challenges in fractional contexts. Therefore, ERPSM is an alternative tool to various series solution methods for solving differential equations of fractional order. Moreover, ERPSM has been capable of solving NFDEs without relying on He's or Adomian's polynomials. Consequently, ERPSM has required significantly fewer computations to solve NFDEs, making it a viable substitute for methods reliant on He's or Adomian polynomials. Additionally, ERPSM has generated series solutions for FNLSM without using the concepts of perturbation, linearization, or discretization, distinguishing it from numerous approximation techniques. Given these results, we have established that our technique is both accurate and simple to use.

In the future, we intend to employ ERPSM to solve both the Nagumo-type equation and evolutionary equations [34,35]. Additionally, we will investigate whether this method can be applied to stochastic problems. If any modifications are required for the method to solve fractional stochastic differential equations, we will work on implementing these amendments.

Author Contributions: Conceptualization, A.M.D., Z.A.K., M.I.L. and A.A.-Q.; methodology, A.M.D., Z.A.K., M.I.L. and A.A.-Q.; software, A.M.D., Z.A.K., M.I.L. and A.A.-Q.; validation, A.M.D., Z.A.K., M.I.L. and A.A.-Q.; formal analysis, A.M.D., Z.A.K., M.I.L. and A.A.-Q.; investigation, A.M.D., Z.A.K., M.I.L. and A.A.-Q.; resources, A.M.D. and Z.A.K.; writing—original draft preparation, A.M.D., Z.A.K. and M.I.L.; writing—review and editing, A.M.D., Z.A.K. and M.I.L.; visualization, A.M.D., Z.A.K. and M.I.L.; funding acquisition, A.M.D., Z.A.K. and A.A.-Q. All authors have read and agreed to the published version of the manuscript.

Funding: Princess Nourah bint Abdulrahman University Researchers Supporting Project number (PNURSP2024R8). Princess Nourah bint Abdulrahman University, Riyadh, Saudi Arabia.

This work was supported by the Deanship of Scientific Research, Vice Presidency for Graduate Studies and Scientific Research, King Faisal University, Saudi Arabia (Project No. GrantA191).

Data Availability Statement: The article contained both data and implementing information.

Conflicts of Interest: The authors declare no conflicts of interest.

Appendix A

The detailed derivations of ϑ_1 , Θ_1 , Ψ_1 , Φ_1 , and Ω_1 are given below.

Firstly, by utilizing $\kappa = 1$ in Equation (13) and κ th-truncated FPS, we obtain the following results:

$$\begin{aligned} \mathcal{Z}Res_1(\vartheta^*(\sigma)) &= \vartheta_1^*(\sigma) - \sigma^2\vartheta_0 - \sigma^\varrho\beta\Omega_1^*(\sigma) + \sigma^\varrho\delta_1\mathcal{Z}[\mathcal{Z}^{-1}[\vartheta_1^*(\sigma)]\mathcal{Z}^{-1}[\Theta_1^*(\sigma)]] + \sigma^\varrho(\zeta_1 + \omega)\vartheta_1^*(\sigma) - \\ &\quad \sigma^\varrho\theta\Phi_1^*(\sigma), \\ \mathcal{Z}Res_1(\Theta^*(\sigma)) &= \Theta_1^*(\sigma) - \sigma^2\Theta_0 + \sigma^\varrho\delta_1\mathcal{Z}[\mathcal{Z}^{-1}[\vartheta_1^*(\sigma)]\mathcal{Z}^{-1}[\Theta_1^*(\sigma)]] + \sigma^\varrho\delta_2\mathcal{Z}[\mathcal{Z}^{-1}[\Psi_1^*(\sigma)]\mathcal{Z}^{-1}[\Theta_1^*(\sigma)]] + \\ &\quad (\zeta_2 + \omega)\sigma^\varrho\Theta_1^*(\sigma), \\ \mathcal{Z}Res_1(\Psi^*(\sigma)) &= \Psi_1^*(\sigma) - \sigma^2\Psi_0 - \sigma^\varrho\delta_2\mathcal{Z}[\mathcal{Z}^{-1}[\Psi_1^*(\sigma)]\mathcal{Z}^{-1}[\Theta_1^*(\sigma)]] + \sigma^\varrho(Y + \zeta_3 + \omega)\Psi_1^*(\sigma), \\ \mathcal{Z}Res_1(\Phi^*(\sigma)) &= \Phi_1^*(\sigma) - \sigma^2\Phi_0 - \sigma^\varrho Y\Psi_1^*(\sigma) + \sigma^\varrho(\theta - \zeta_4 + \omega)\Phi_1^*(\sigma), \\ \mathcal{Z}Res_1(\Omega^*(\sigma)) &= \Omega_1^*(\sigma) - \sigma^2\Omega_0 + \sigma^\varrho(\beta - \omega)\Omega_1^*(\sigma) + \sigma^\varrho(\zeta_1\vartheta_1^*(\sigma) + \zeta_2\Theta_1^*(\sigma) - \zeta_3\Psi_1^*(\sigma) + \zeta_4\Phi_1^*(\sigma)). \end{aligned} \quad (A1)$$

Further, $\vartheta_1^*(\sigma) = \vartheta_0\sigma^2 + \vartheta_1\sigma^{2+\varphi}$, $\Theta_1^*(\sigma) = \Theta_0\sigma^2 + \Theta_1\sigma^{2+\varphi}$, $\Psi_1^*(\sigma) = \Psi_0\sigma^2 + \Psi_1\sigma^{2+\varphi}$, $\Phi_1^*(\sigma) = \Phi_0\sigma^2 + \Phi_1\sigma^{2+\varphi}$, and $\Omega_1^*(\sigma) = \Omega_0\sigma^2 + \Omega_1\sigma^{2+\varphi}$,

By utilizing the above-obtained results, we obtain the following outcomes:

$$\begin{aligned}
 {}_{eq}(A2) \mathcal{Z}Res_1(\vartheta^*(\sigma)) &= (\vartheta_0\sigma^2 + \vartheta_1\sigma^{2+\varphi}) - \vartheta_0\sigma^2 - \sigma^\varphi\beta(\Omega_0\sigma^2 + \Omega_1\sigma^{2+\varphi}) + \sigma^\varphi\delta_1\mathcal{Z}[\mathcal{Z}^{-1}[\vartheta_0\sigma^2 + \vartheta_1\sigma^{2+\varphi}] \\
 &\quad \mathcal{Z}^{-1}[\Theta_0\sigma^2 + \Theta_1\sigma^{2+\varphi}]] + \sigma^\varphi(\zeta_1 + \omega)(\vartheta_0\sigma^2 + \vartheta_1\sigma^{2+\varphi}) - \sigma^\varphi\theta(\Phi_0\sigma^2 + \Phi_1\sigma^{2+\varphi}), \\
 \mathcal{Z}Res_1(\Theta^*(\sigma)) &= (\Theta_0\sigma^2 + \Theta_1\sigma^{2+\varphi}) - \sigma^2\Theta_0 + \sigma^\varphi\delta_1\mathcal{Z}[\mathcal{Z}^{-1}[\vartheta_0\sigma^2 + \vartheta_1\sigma^{2+\varphi}]\mathcal{Z}^{-1}[\Theta_0\sigma^2 + \Theta_1\sigma^{2+\varphi}]] + \\
 &\quad \sigma^\varphi\delta_2\mathcal{Z}[\mathcal{Z}^{-1}[\Psi_0\sigma^2 + \Psi_1\sigma^{2+\varphi}]\mathcal{Z}^{-1}[\Theta_0\sigma^2 + \Theta_1\sigma^{2+\varphi}]] + (\zeta_2 + \omega)\sigma^\varphi(\Theta_0\sigma^2 + \Theta_1\sigma^{2+\varphi}), \\
 \mathcal{Z}Res_1(\Psi^*(\sigma)) &= \Psi_0 + \Psi_1\sigma^{2+\varphi} - \sigma^2\Psi_0 - \sigma^\varphi\delta_2\mathcal{Z}[\mathcal{Z}^{-1}[\Psi_0\sigma^2 + \Psi_1\sigma^{2+\varphi}]\mathcal{Z}^{-1}[\Theta_0 + \Theta_1\sigma^{2+\varphi}]] + \\
 &\quad \sigma^\varphi(Y + \zeta_3 + \omega)(\Psi_0\sigma^2 + \Psi_1\sigma^{2+\varphi}), \tag{A2} \\
 \mathcal{Z}Res_1(\Phi^*(\sigma)) &= \Phi_0\sigma^2 + \Phi_1\sigma^{2+\varphi} - \sigma^2\Phi_0 - \sigma^\varphi Y(\Psi_0\sigma^2 + \Psi_1\sigma^{2+\varphi}) + \sigma^\varphi(\theta - \zeta_4 + \omega)(\Phi_0\sigma^2 + \Phi_1\sigma^{2+\varphi}), \\
 \mathcal{Z}Res_1(\Omega^*(\sigma)) &= \Omega_0\sigma^2 + \Omega_1\sigma^{2+\varphi} - \sigma^2\Omega_0 + \sigma^\varphi(\beta - \omega)(\Omega_0\sigma^2 + \Omega_1\sigma^{2+\varphi}) + \sigma^\varphi(\zeta_1(\vartheta_0\sigma^2 + \vartheta_1\sigma^{2+\varphi}) + \\
 &\quad \zeta_2(\Theta_0\sigma^2 + \Theta_1\sigma^{2+\varphi}) - \zeta_3(\Psi_0\sigma^2 + \Psi_1\sigma^{2+\varphi}) + \zeta_4(\Phi_0\sigma^2 + \Phi_1\sigma^{2+\varphi})).
 \end{aligned}$$

By using values of $\mathcal{Z}Res_1(\vartheta^*(\sigma))$, $\mathcal{Z}Res_1(\Theta^*(\sigma))$, $\mathcal{Z}Res_1(\Psi^*(\sigma))$, $\mathcal{Z}Res_1(\Phi^*(\sigma))$, and $\mathcal{Z}Res_1(\Omega^*(\sigma))$ in Equation (14), we obtain the desired values of ϑ_1 , Θ_1 , Ψ_1 , Φ_1 , and Ω_1 , as provided in Equation (15). In the same way, we obtained the remaining coefficient of FPS by repeating the procedure for $\kappa = 2, 3, 4, 5$, and 6. The values are provided in Equations (16)–(20).

References

1. Monje, C.A.; Chen, Y.; Vinagre, B.M.; Xue, D.; Feliu-Batlle, V. *Fractional-Order Systems and Controls: Fundamentals and Applications*; Springer Science Business Media: Berlin/Heidelberg, Germany, 2010.
2. Samko, S. Fractional integration and differentiation of variable order: An overview. *Nonlinear Dyn.* **2013**, *71*, 653–662. [\[CrossRef\]](#)
3. Abu-Ghuwaleh; M.; Saadeh, R. New definitions of fractional derivatives and integrals for complex analytic functions. *Arab. J. Basic Appl. Sci.* **2023**, *30*, 675–690. [\[CrossRef\]](#)
4. Zhou, P.; Ma, J.; Tang, J. Clarify the physical process for fractional dynamical systems. *Nonlinear Dyn.* **2020**, *100*, 2353–2364. [\[CrossRef\]](#)
5. Arfan, M.; Lashin, M.M.; Sunthrayuth, P.; Shah, K.; Ullah, A.; Iskakova, K.; Abdeljawad, T. On nonlinear dynamics of COVID-19 disease model corresponding to nonsingular fractional order derivative. *Med. Biol. Eng. Comput.* **2022**, *60*, 3169–3185. [\[CrossRef\]](#) [\[PubMed\]](#)
6. Mangal, S.; Misra, O.P.; Dhar, J. SIRS epidemic modeling using fractional-ordered differential equations: Role of fear effect. *Int. J. Biomath.* **2024**, *17*, 2350044. [\[CrossRef\]](#)
7. Singh, H.; Baleanu, D.; Singh, J.; Dutta, H. Computational study of fractional order smoking model. *Chaos Solit. Fract.* **2021**, *142*, 110440. [\[CrossRef\]](#)
8. Alrabaiah, H.; Zeb, A.; Alzahrani, E.; Shah, K. Dynamical analysis of fractional-order tobacco smoking model containing snuffing class. *Alex. Eng. J.* **2021**, *60*, 3669–3678. [\[CrossRef\]](#)
9. Hassani, H.; Machado, J.T.; Avazzadeh, Z.; Naraghirad, E.; Mehrabi, S. Optimal solution of the fractional-order smoking model and its public health implications. *Nonlinear Dyn.* **2022**, *108*, 2815–2831. [\[CrossRef\]](#)
10. Liu, P.; Munir, T.; Cui, T.; Din, A.; Wu, P. Mathematical assessment of the dynamics of the tobacco smoking model: An application of fractional theory. *AIMS Math.* **2022**, *7*, 7143–7165. [\[CrossRef\]](#)
11. Swartz, J.B. Use of a Multistage Model to Predict Time Trends in Smoking Induced Lung Cancer. *J. Epidemiol. Community Health* **1992**, *46*, 311–315. [\[CrossRef\]](#)
12. Brauer, F.; Castillo-Chavez, C. *Mathematical Models in Population Biology and Epidemiology*; Springer: Berlin/Heidelberg, Germany, 2001.
13. Zaman, G. Optimal campaign in the smoking dynamics. *Comput. Math. Methods Med.* **2011**, *2011*, 163834. [\[CrossRef\]](#)
14. Li, C.; Zhang, H.; Yang, X. A New Nonlinear Compact Difference Scheme for a Fourth-Order Nonlinear Burgers Type Equation with a Weakly Singular Kernel. *J. Appl. Math. Comput.* **2024**, *2024*, 1–33. [\[CrossRef\]](#)
15. Shi, Y.; Yang, X. Pointwise error estimate of conservative difference scheme for supergeneralized viscous Burgers' equation. *Electron. Res. Arch.* **2024**, *32*, 1471–1497. [\[CrossRef\]](#)
16. Wang, W.; Zhang, H.; Zhou, Z.; Yang, X. A Fast Compact Finite Difference Scheme for the Fourth-Order Diffusion-Wave Equation. *Inter. J. Comput. Math.* **2024**, *101*, 170–193. [\[CrossRef\]](#)
17. Shi, Y.; Yang, X. A time two-grid difference method for nonlinear generalized viscous Burgers' equation. *J. Math. Chem.* **2024**, *2014*, 1–34. [\[CrossRef\]](#)
18. Liaqat, M. I.; Khan, A.; Akgül, A. Adaptation on power series method with conformable operator for solving fractional order systems of nonlinear partial differential equations. *Chaos Solit. Fract.* **2022**, *157*, 111984. [\[CrossRef\]](#)
19. Zaky, M.A. An accurate spectral collocation method for nonlinear systems of fractional differential equations and related integral equations with nonsmooth solutions. *Appl. Numer. Math.* **2020**, *154*, 205–222. [\[CrossRef\]](#)
20. Jajarmi, A.; Baleanu, D. A new iterative method for the numerical solution of high-order non-linear fractional boundary value problems. *Front. Phys.* **2020**, *8*, 220. [\[CrossRef\]](#)

21. Khalid, N.; Abbas, M.; Iqbal, M.K.; Singh, J.; Ismail, A.I.M. A computational approach for solving time fractional differential equation via spline functions. *Alex. Eng. J.* **2020**, *59*, 3061–3078. [[CrossRef](#)]
22. Babaei, A.; Jafari, H.; Banihashemi, S. Numerical solution of variable order fractional nonlinear quadratic integro-differential equations based on the sixth-kind Chebyshev collocation method. *J. Comput. Appl. Math.* **2020**, *377*, 112908. [[CrossRef](#)]
23. Li, D.; Sun, W.; Wu, C. A novel numerical approach to time-fractional parabolic equations with nonsmooth solutions. *Numer. Math. Theory Methods Appl.* **2021**, *14*, 355–376.
24. Haq, F.; Shah, K.; ur Rahman, G.; Shahzad, M. Numerical solution of fractional order smoking model via Laplace Adomian decomposition method. *Alex. Eng. J.* **2018**, *57*, 1061–1069. [[CrossRef](#)]
25. Mahdy, A.M.S.; Sweilam, N.H.; Higazy, M. Approximate solution for solving nonlinear fractional order smoking model. *Alex. Eng. J.* **2020**, *59*, 739–752. [[CrossRef](#)]
26. Pavani, K.; Raghavendar, K. A novel technique to study the solutions of time fractional nonlinear smoking epidemic model. *Sci. Rep.* **2024**, *14*, 4159. [[CrossRef](#)] [[PubMed](#)]
27. Khan, S.A.; Shah, K.; Zaman, G.; Jarad, F. Existence Theory and Numerical Solutions to Smoking Model under Caputo-Fabrizio Fractional Derivative. *Chaos: An Interdiscip. J. Nonlinear Sci.* **2019**, *29*, 013128.
28. Veerasha, P.; Prakasha, D.G.; Baskonus, H.M. Solving smoking epidemic model of fractional order using a modified homotopy analysis transform method. *Math. Sci.* **2019**, *13*, 115–128. [[CrossRef](#)]
29. Gunerhan, H.; Rezazadeh, H.; Adel, W.; Hatami, M.; Sagayam, K.M.; Emadifar, H.; Hamoud, A.A. Analytical approximate solution of fractional order smoking epidemic model. *Adv. Mech. Eng.* **2022**, *14*, , 1–11. [[CrossRef](#)]
30. Mohammed, O.H.; Salim, H.A. Computational methods based laplace decomposition for solving nonlinear system of fractional order differential equations. *Alex. Eng. J.* **2018**, *57*, 3549–3557. [[CrossRef](#)]
31. He, W.; Chen, N.; Dassios, I.; Shah, N.A.; Chung, J.D. Fractional system of Korteweg-De Vries equations via Elzaki transform. *Mathematics* **2021**, *9*, 673. [[CrossRef](#)]
32. Liaqat, M.I.; Akgül, A.; Bayram, M. Series and Closed Form Solution of Caputo Time-Fractional Wave and Heat Problems with the Variable Coefficients by a Novel Approach. *Opt. Quant. Electron.* **2024**, *56*, 203. [[CrossRef](#)]
33. Liaqat, M.I.; Khan, A.; Akgül, A.; Ali, M.S. A Novel Numerical Technique for Fractional Ordinary Differential Equations with Proportional Delay. *J. Funct. Spaces* **2022**, *2022*, 1–21. [[CrossRef](#)]
34. Yang, X.; Zhang, Z. On conservative, positivity preserving, nonlinear FV scheme on distorted meshes for the multi-term nonlocal Nagumo-type equations. *Appl. Math. Lett.* **2024**, *150*, 108972. [[CrossRef](#)]
35. Yang, X.; Qiu, W.; Chen, H.; Zhang, H. Second-order BDF ADI Galerkin finite element method for the evolutionary equation with a nonlocal term in three-dimensional space. *Appl. Numer. Math.* **2022**, *172*, 497–513. [[CrossRef](#)]

Disclaimer/Publisher’s Note: The statements, opinions and data contained in all publications are solely those of the individual author(s) and contributor(s) and not of MDPI and/or the editor(s). MDPI and/or the editor(s) disclaim responsibility for any injury to people or property resulting from any ideas, methods, instructions or products referred to in the content.